Toroidal vorticity in light-on-heavy collisions: Event-by-event simulations

Mike Lisa
The Ohio State University

this talk → light-on-heavy
Phys. Rev. **C104** (2021) 011901
Phys. Rev. **C110** (2024) 054908

jet-through-plasma ← Talk by Cicero Muncinelli
Phys. Lett. **B820** (2021) 136500
Phys. Rev. **C109** (2024) 014905

João Prado Barbon, David D. Chinellato, MAL, Vítor H. Ribeiro, Willian M. Serenone, Chun Shen, Jun Takahashi, Giorgio Torrieri
(3C Collaboration)

UNICAMP THE OHIO STATE UNIVERSITY WAYNE STATE

Outline

- Vorticity patterns in seen and not-yet seen
  - global / longitudinal / circular / **toroidal**

- Vortical toroids (“smoke rings”) in small-on-large collisions
  - simulations with smooth IC
  - simulations with e-by-e fluctuating IC
  - possibility to measure in p+A collisions in final RHIC run

- Summary

Polarization patterns in heavy ion collisions- seen

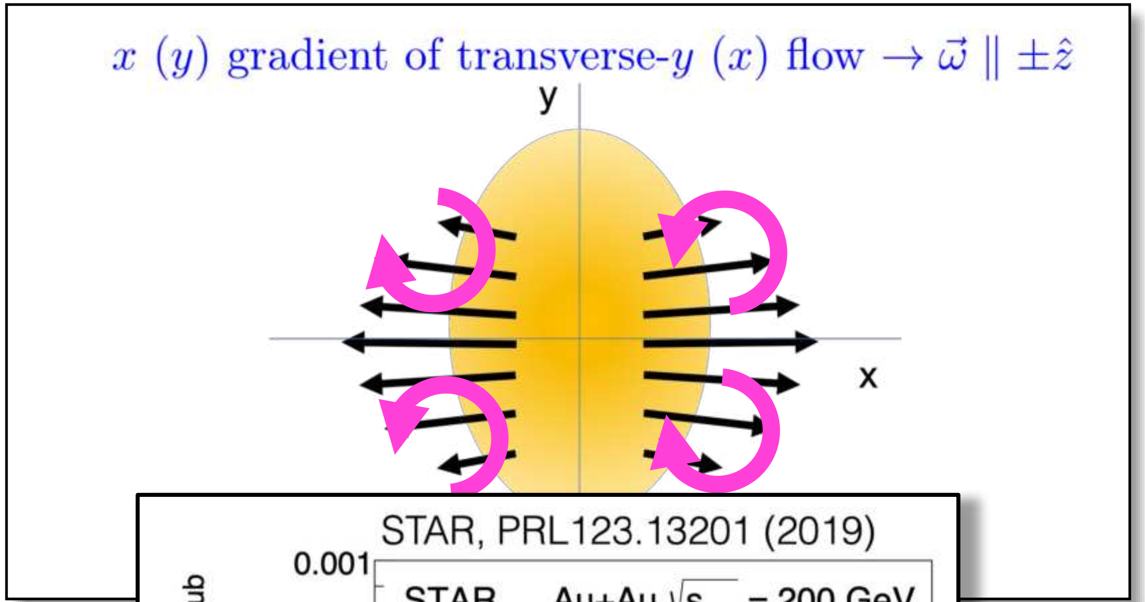

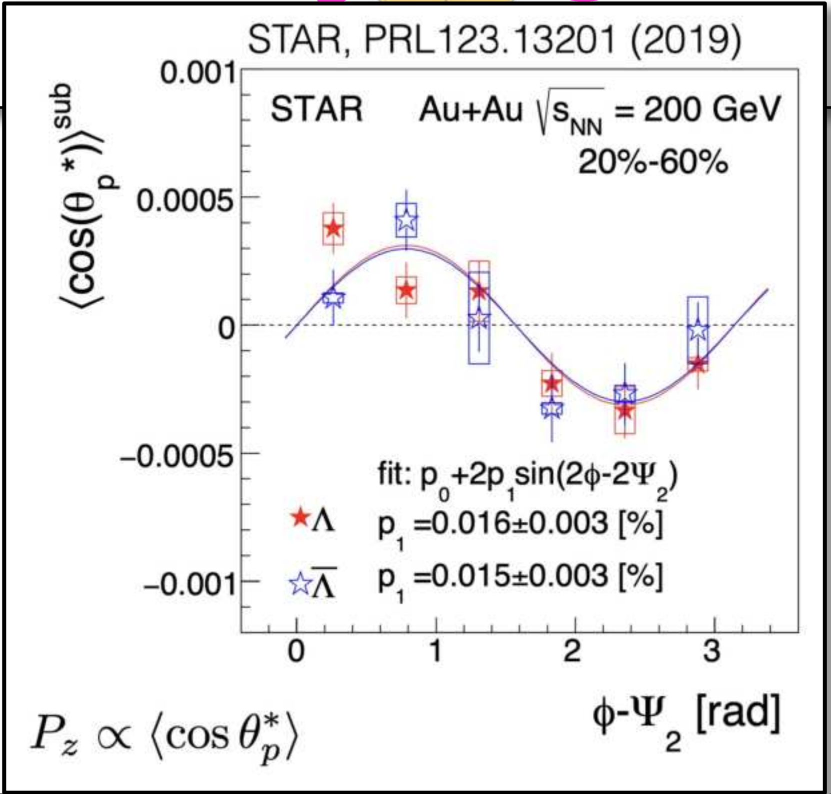

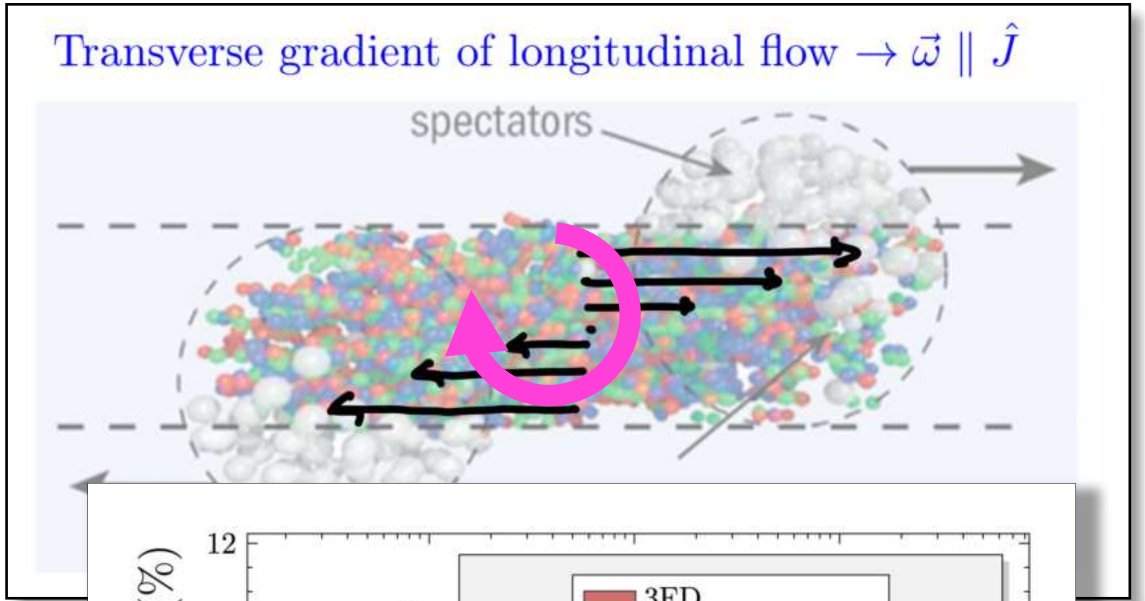

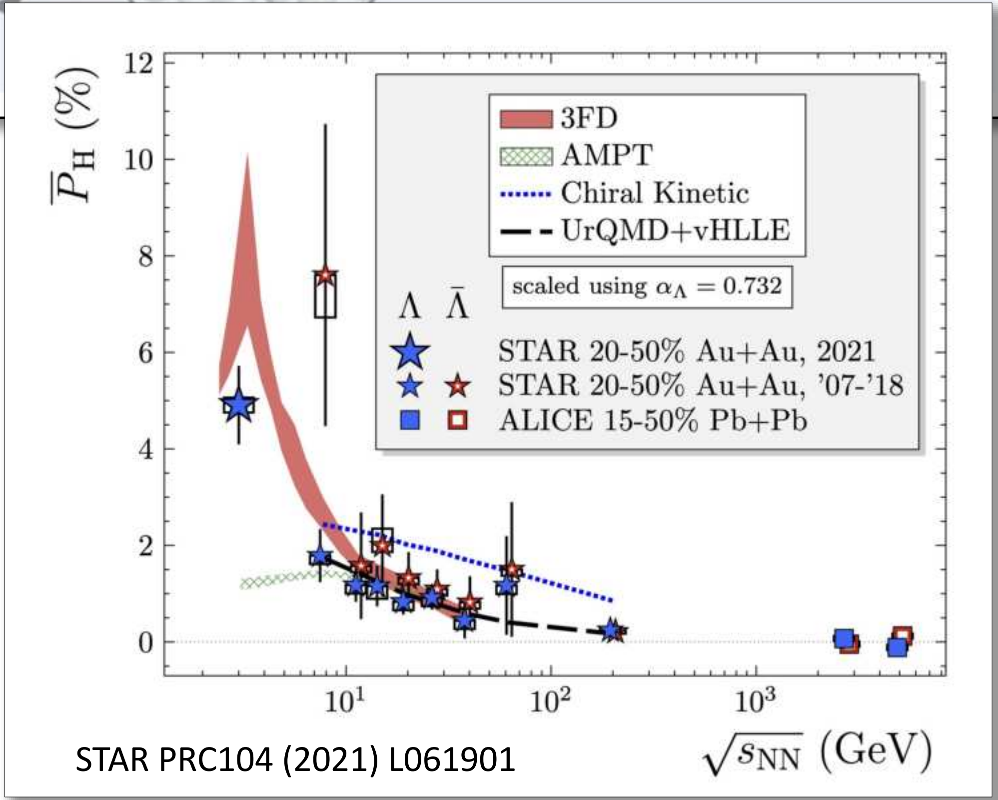

STAR PRC104 (2021) L061901

Polarization patterns in heavy ion collisions- seen & not yet seen

x (y) gradient of transverse-y (x) flow $\rightarrow \vec{\omega} \parallel \pm\hat{z}$

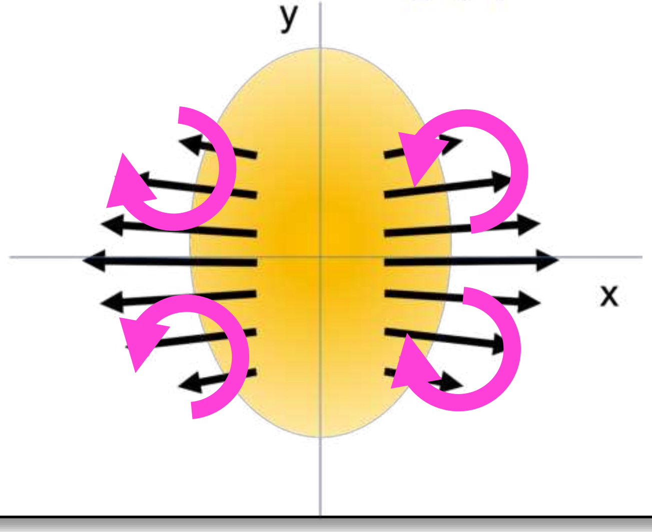

Transverse gradient of longitudinal flow $\rightarrow \vec{\omega} \parallel \hat{J}$

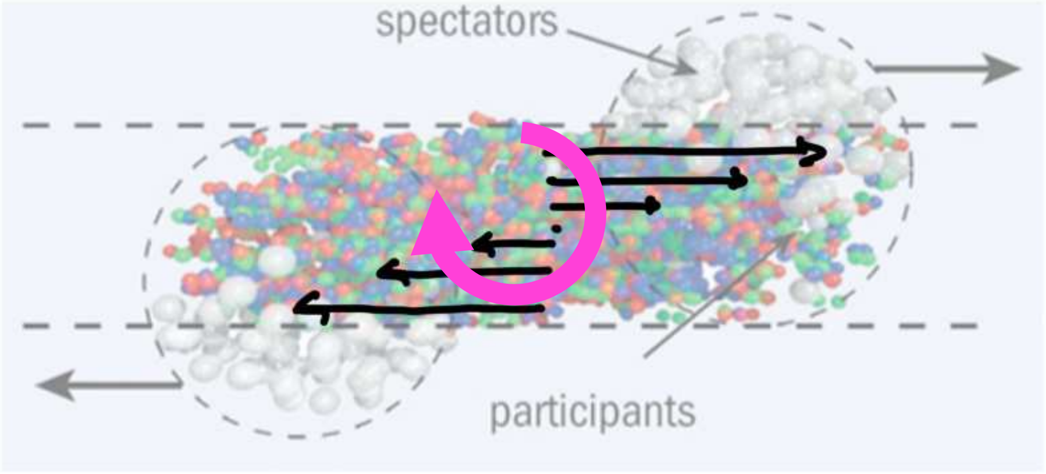

Longitudinal gradient of transverse flow (& temp.) $\rightarrow$ circular structure of $\vec{\omega}$

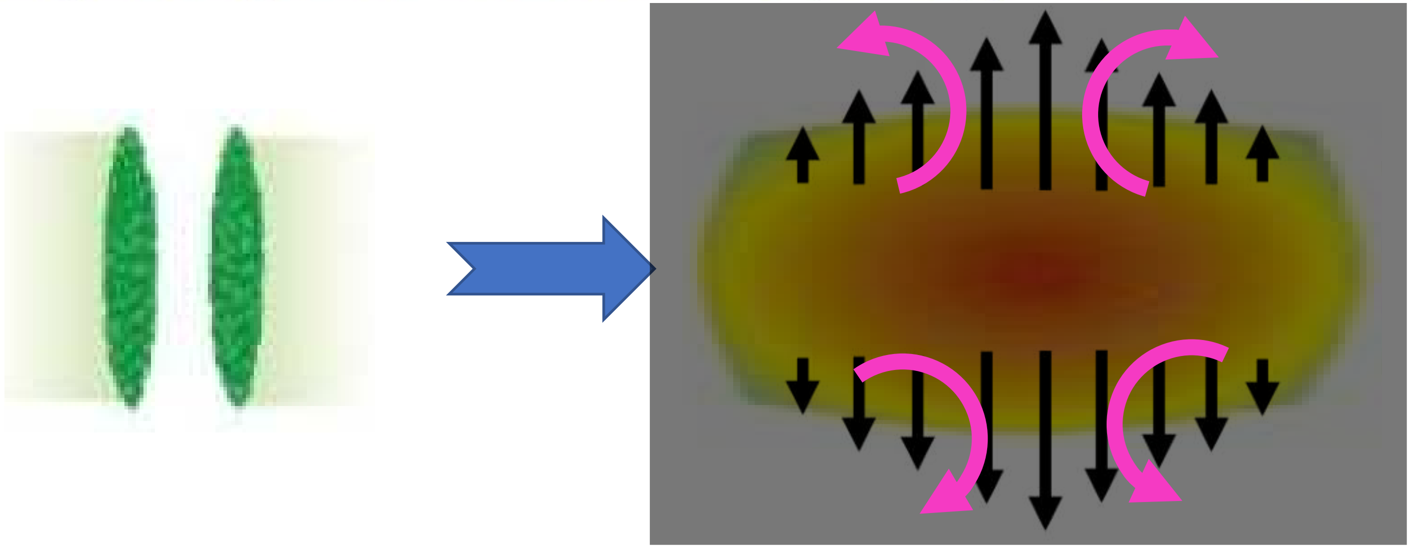

$\vec{\omega} \parallel \vec{p} \times \vec{z}$

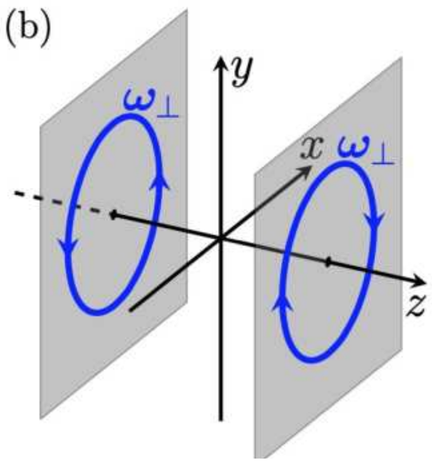

Xia, Li, Tang, Wang PRC 98, 024905 (2018)

Polarization patterns in heavy ion collisions- seen & not yet seen

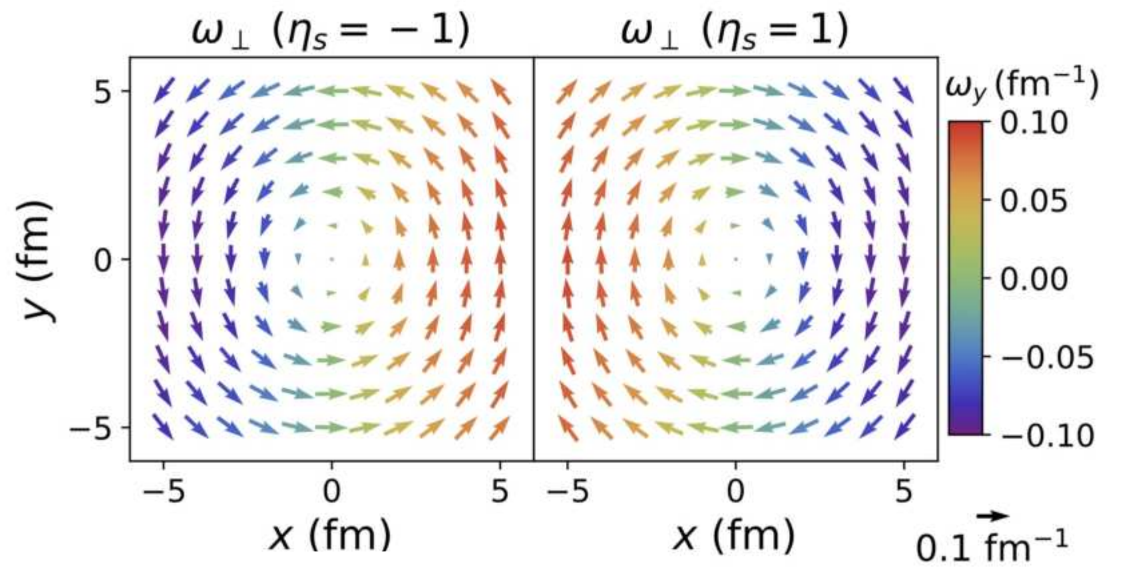

Xia, Li, Tang, Wang PRC 98, 024905 (2018)

quantifying circular polarization structure

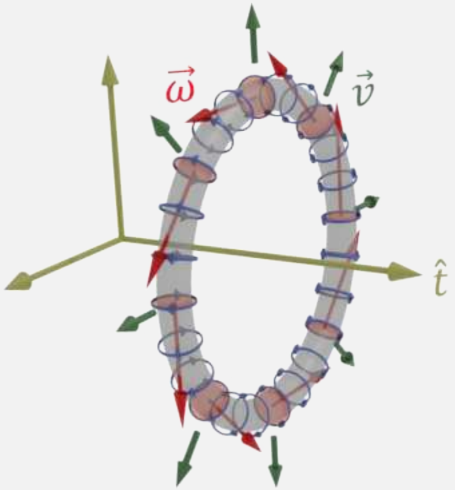

$$\overline{\mathcal{R}}^{\hat{t}}_{\mathrm{NR}} \equiv \left\langle \frac{\vec{\omega}_{\mathrm{NR}} \cdot (\hat{t} \times \vec{v}_{\mathrm{cell}})}{|\hat{t} \times \vec{v}_{\mathrm{cell}}|} \right\rangle_\phi$$

$$\mathcal{R}^{\hat{t}}_{\mathrm{fluid}} \equiv \frac{\epsilon^{\mu\nu\rho\sigma}\Omega_\mu n_\nu \hat{t}_\rho u_\sigma}{|\epsilon^{\mu\nu\rho\sigma} n_\nu \hat{t}_\rho u_\sigma|}$$

PRC104 (2021) 011901

Longitudinal gradient of transverse flow (& temp.) $\rightarrow$ circular structure of $\vec{\omega}$

$\vec{\omega} \parallel \vec{p} \times \vec{z}$

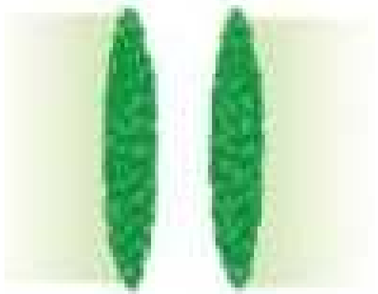

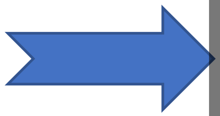

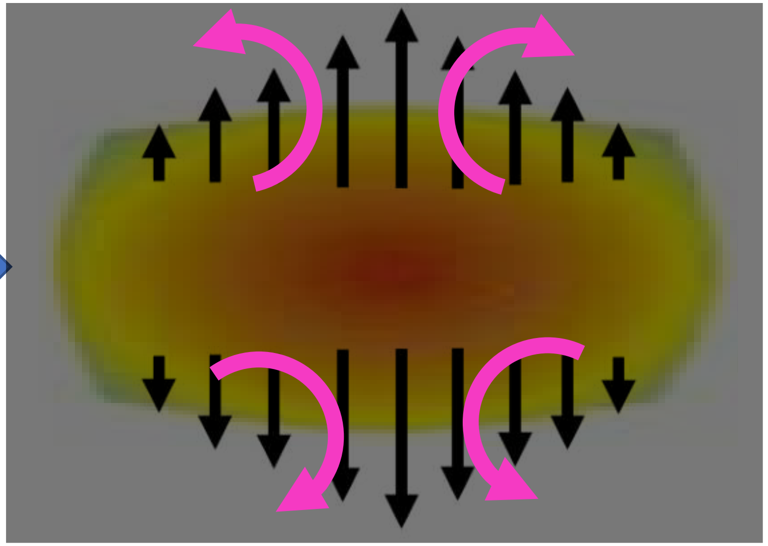

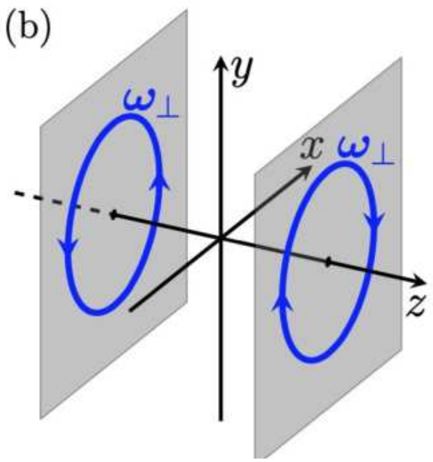

Xia, Li, Tang, Wang PRC 98, 024905 (2018)

PRC104 (2021) 011901

Development of circular vorticity in MUSIC

Au+Au at 200 GeV Bjorken flow profile

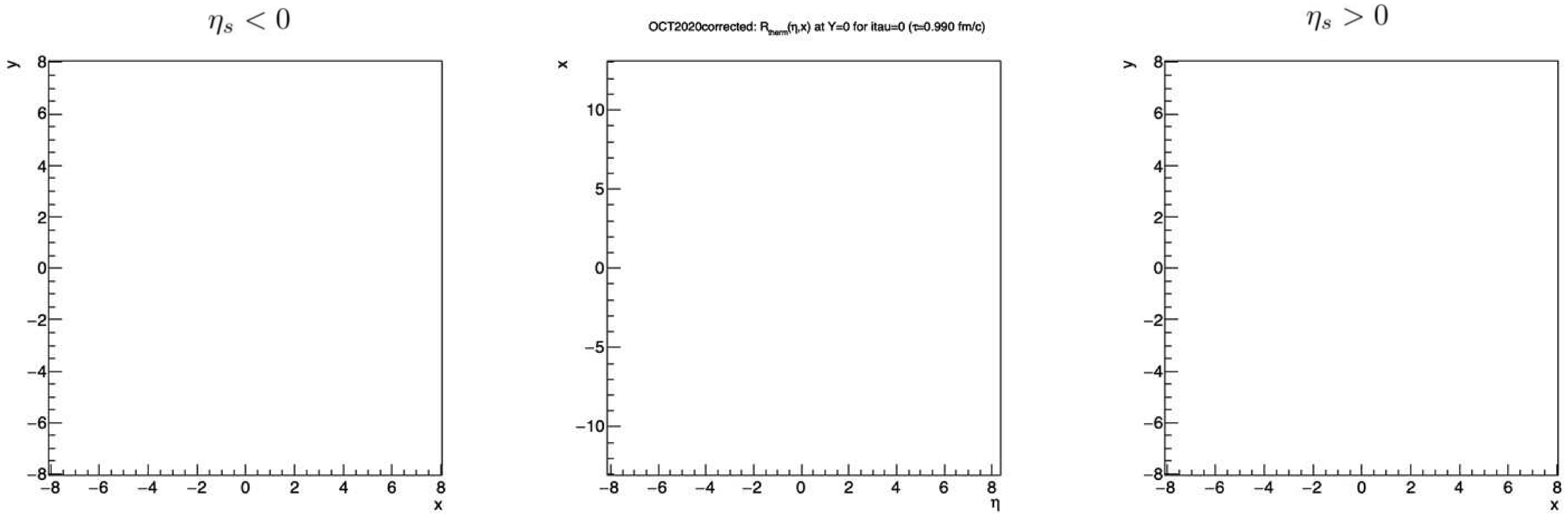

$\vec{\omega}$ $\vec{u}_{\rm cell}$

color axis: $\overline{\mathcal{R}}^{\hat{t}}_{\rm NR} \equiv \left\langle \frac{\vec{\omega}_{\rm NR}\cdot(\hat{t}\times\vec{v}_{\rm cell})}{|\hat{t}\times\vec{v}_{\rm cell}|} \right\rangle_\phi$ ➡ $\mathcal{R}^{\hat{t}}_{\rm fluid} \equiv \frac{\epsilon^{\mu\nu\rho\sigma}\Omega_\mu n_\nu \hat{t}_\rho u_\sigma}{|\epsilon^{\mu\nu\rho\sigma}n_\nu \hat{t}_\rho u_\sigma|}$

MUSIC hydrodynamics, with baryon currents
Schenke, Jeon, Gale PRC82 (2010) 014903
Schenke, Shen, Tribedy PRC102 (2020) 044905

Vorticity "of the flow field"

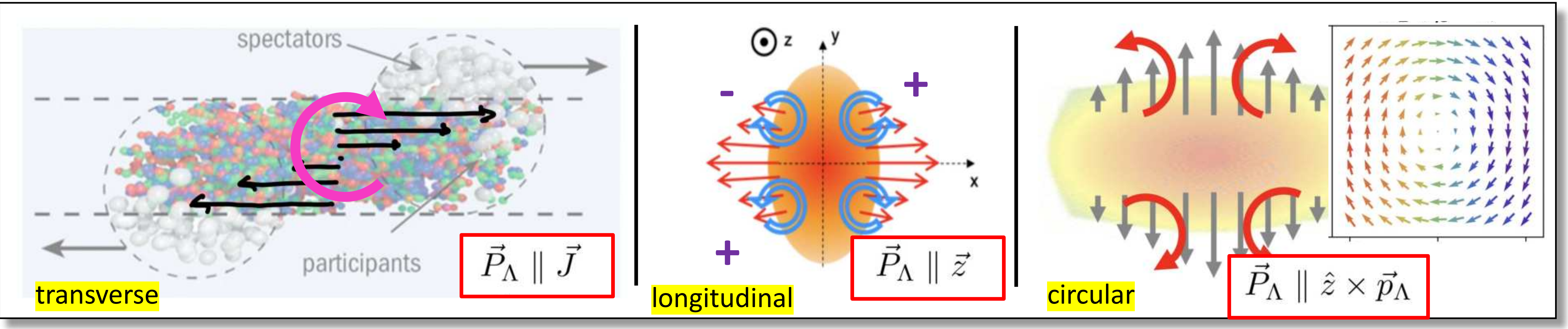

Vorticity toroids visible *due to* transverse flow

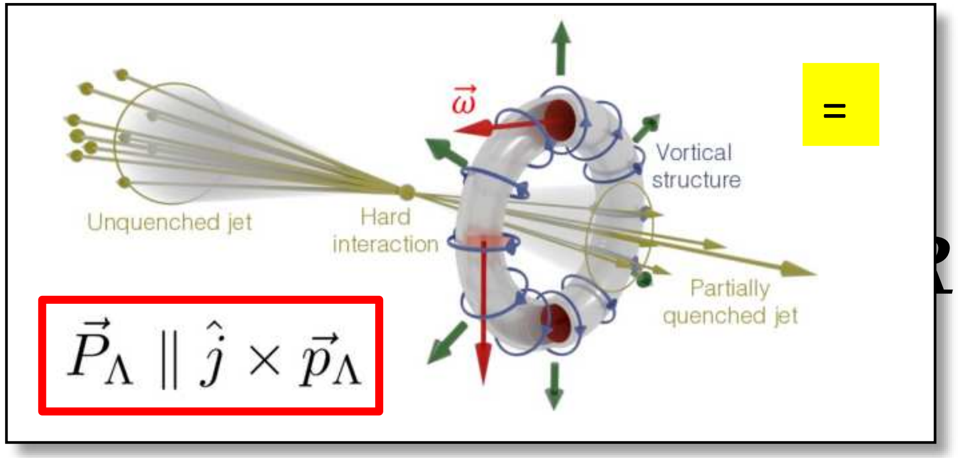

$$R^t_\Lambda = \left\langle \frac{\vec{P}_\Lambda \cdot (\hat{t} \times \vec{p})}{|\hat{t} \times \vec{p}|} \right\rangle$$

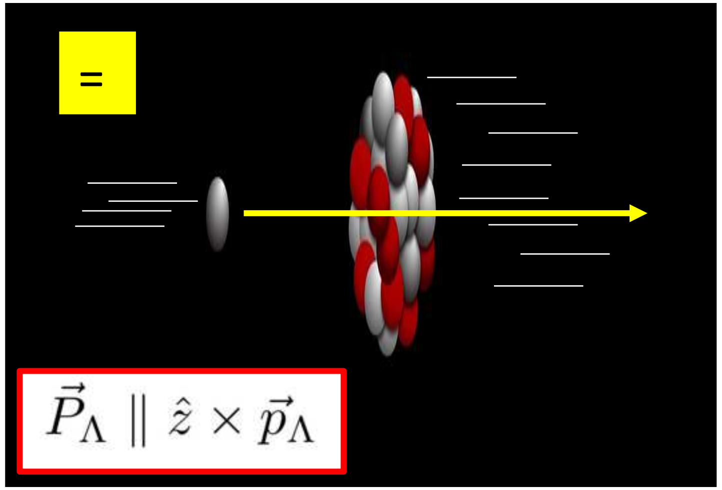

Talk Wed by C. Muncinelli

Like an armor-piercing shell

brief fluid-like behavior

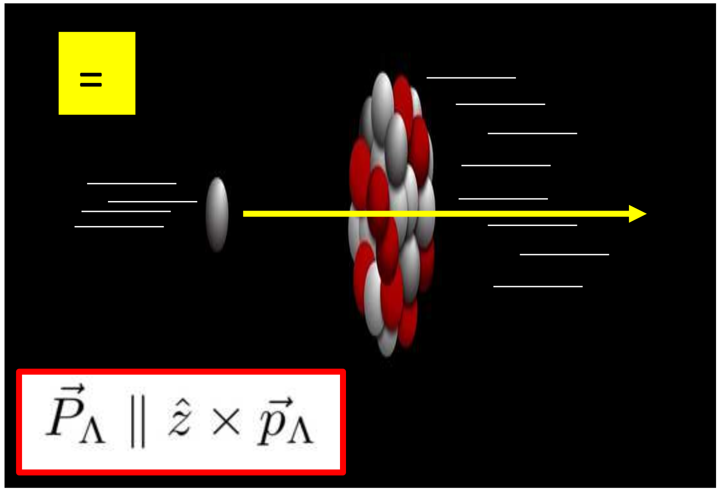

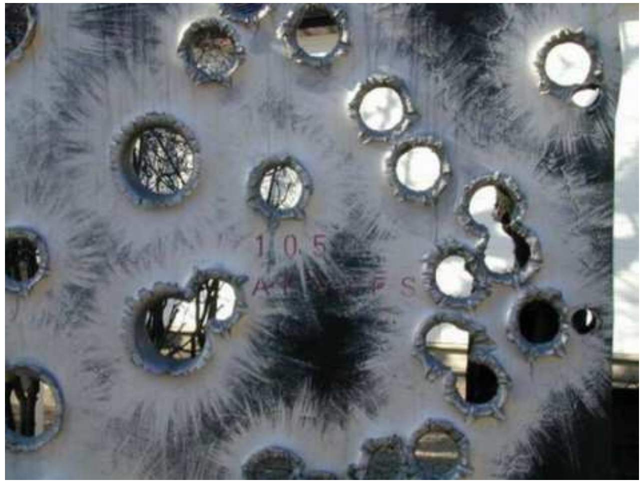

Hydronamization during penetration?

Would provide novel evidence of "smallest droplet of QGP" and its formation

Helmholtz (1867): Persistent vortical toroids (smoke rings) are quintessential fluid behavior in response to a localized disturbance

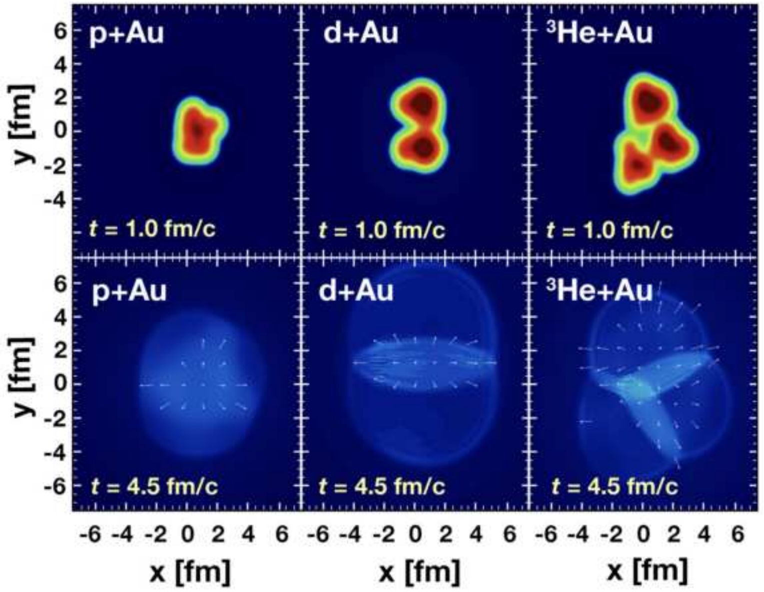

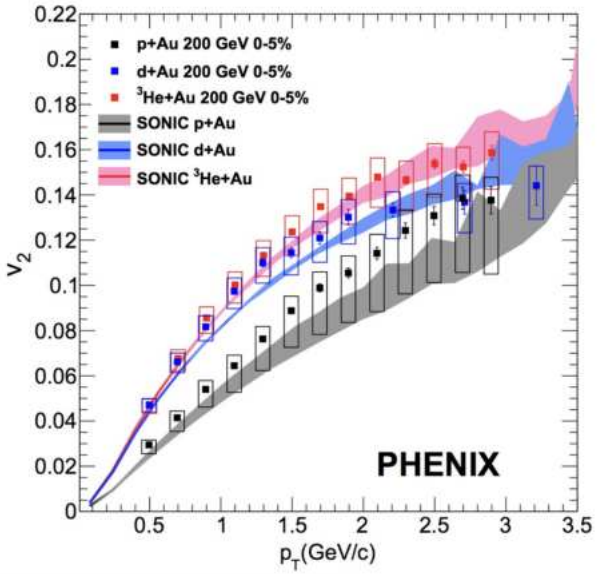

Initial state

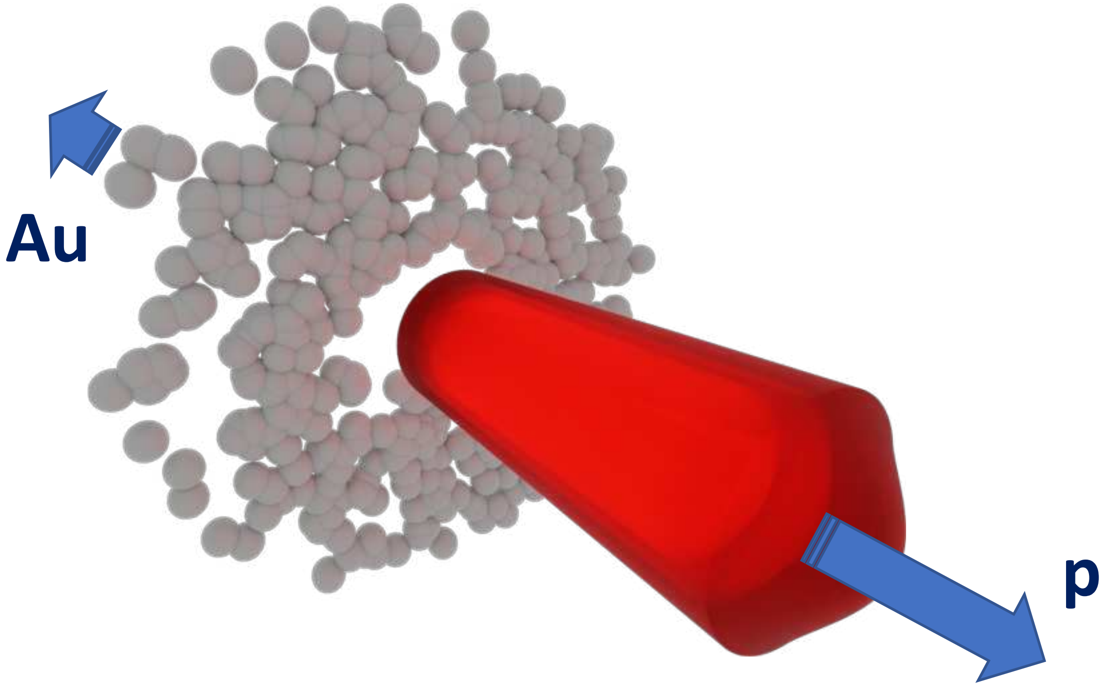

Initial state

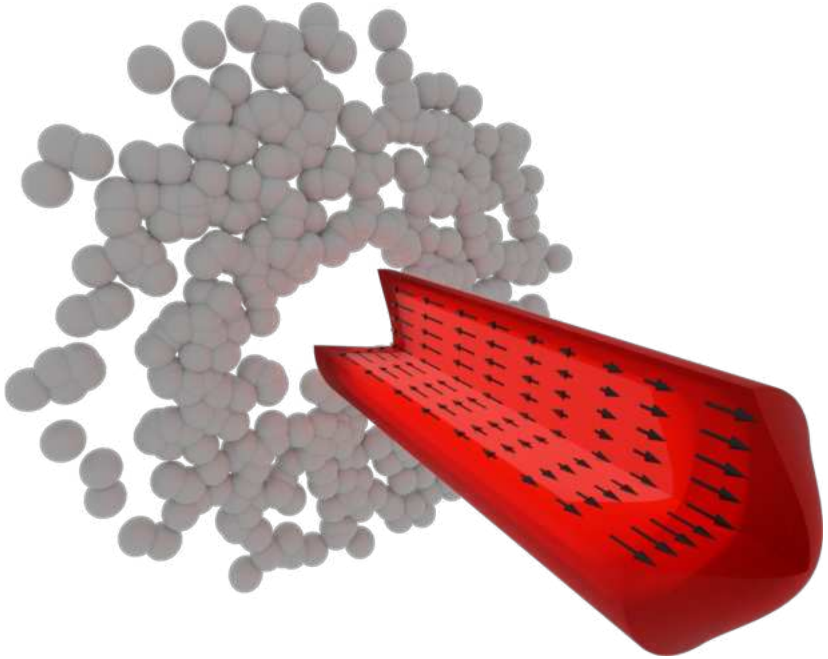

(a) Bjorken flow profile: $u_z = \eta_s$

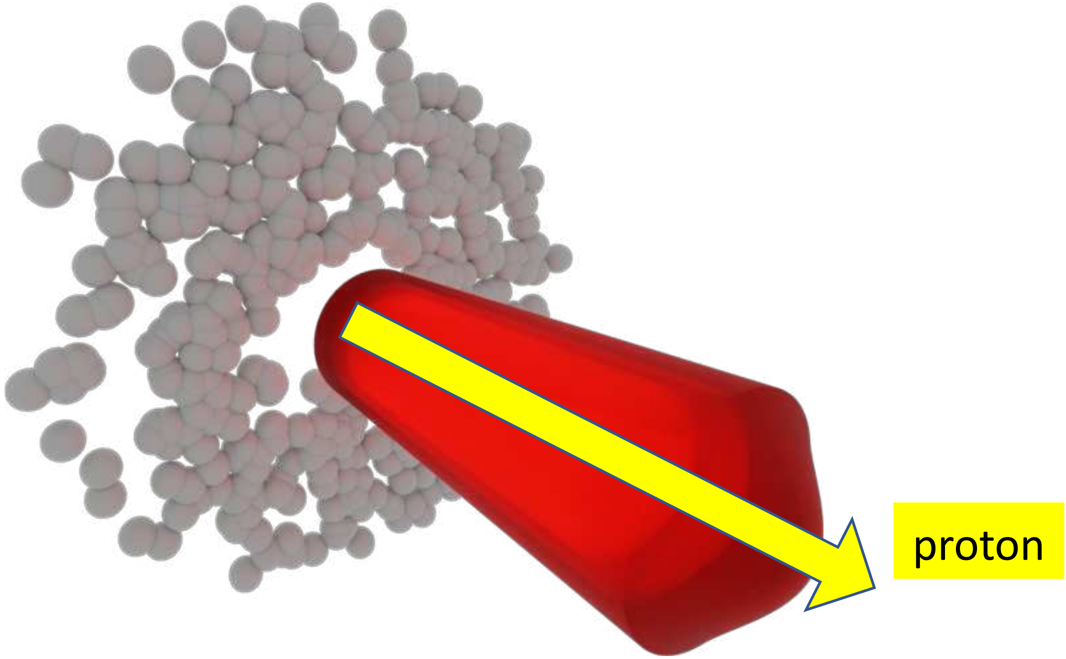

Initial state

Phys. Rev. **C104** (2021) 011901
Phys. Rev. **C110** (2024) 054908

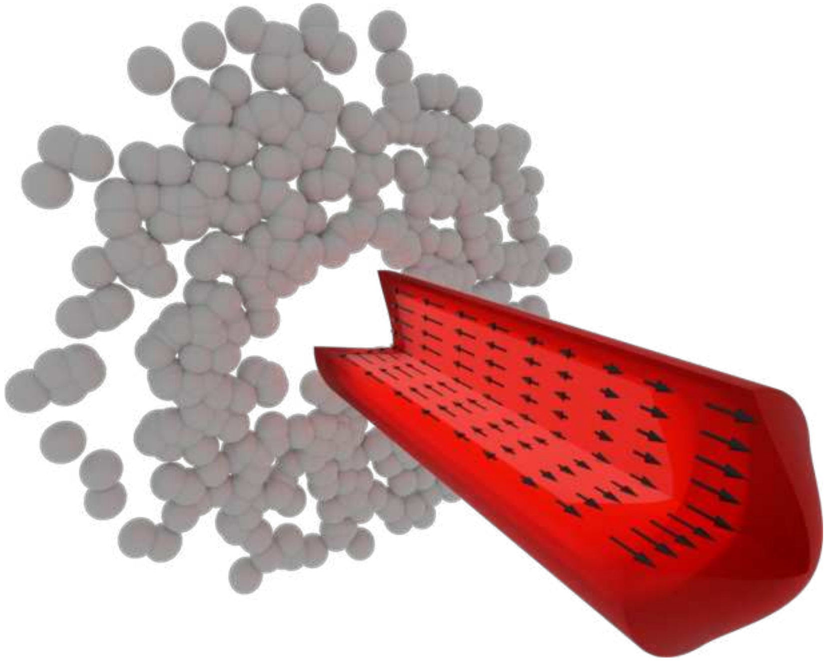

(a) Bjorken flow profile: $u_z = \eta_s$

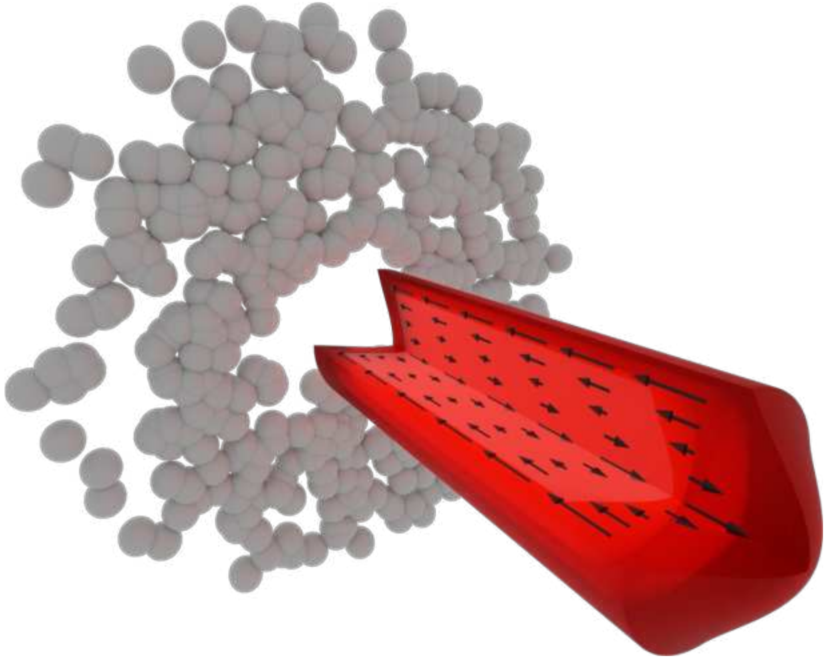

(b) Matter-overlap flow profile

Initial state

Phys. Rev. **C104** (2021) 011901
Phys. Rev. **C110** (2024) 054908

EM tensor
$$T^{\tau\tau} = e(\vec{x}_\perp, \eta_s)\cosh(f y_{\rm CM}(\vec{x}_\perp))$$
$$T^{\tau\eta} = \frac{1}{\tau_0} e(\vec{x}_\perp, \eta_s)\sinh(f y_{\rm CM}(\vec{x}_\perp))$$

where
$$y_{\rm CM}(\vec{x}_\perp) = \text{arctanh}\left[\frac{T_A - T_B}{T_A + T_B}\tanh(y_{\rm beam})\right]$$

MUSIC [1] hydro with Lattice EoS [2]

T_A , T_B are nuclear thickness functions at $x_\perp$
- smooth or e-by-e fluctuating [3]

[1] PRC102 (2020) 014909
[2] PRC82 (2010) 014903
[3] PRC102 (2020) 044905

f=0

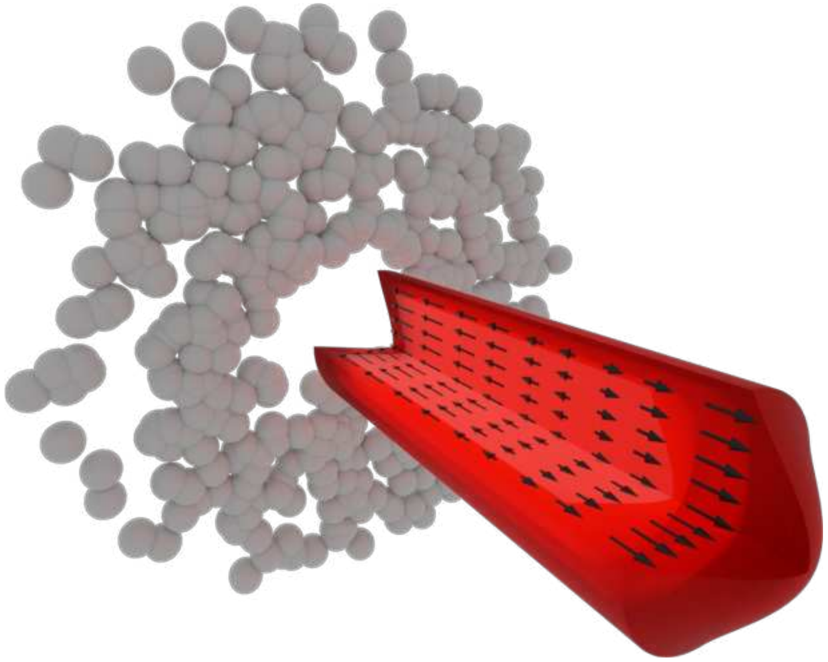

(a) Bjorken flow profile: $u_z = \eta_s$

f=1

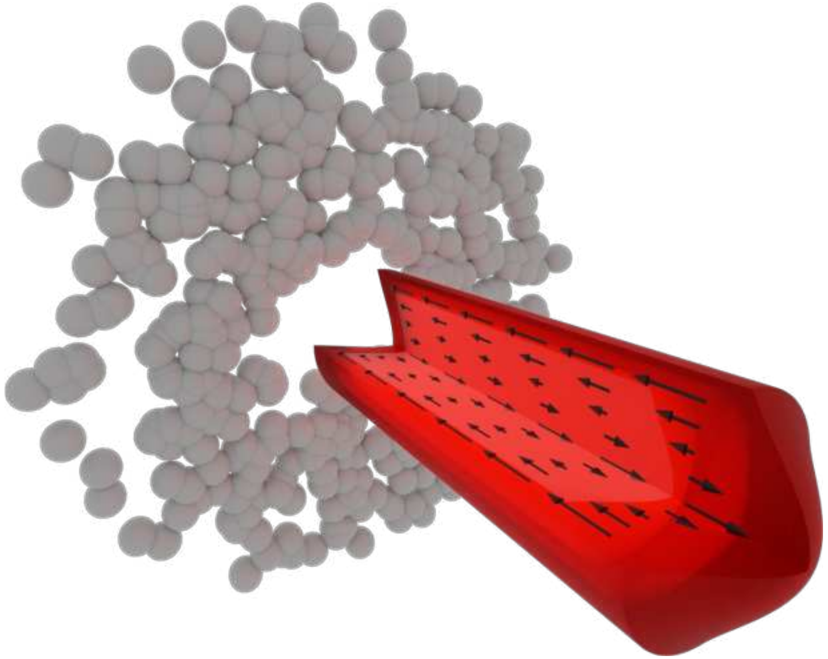

(b) Matter-overlap flow profile

Initial state

Phys. Rev. **C104** (2021) 011901
Phys. Rev. **C110** (2024) 054908

EM tensor
$$T^{\tau\tau} = e(\vec{x}_\perp, \eta_s)\cosh(f y_{\rm CM}(\vec{x}_\perp))$$
$$T^{\tau\eta} = \frac{1}{\tau_0} e(\vec{x}_\perp, \eta_s)\sinh(f y_{\rm CM}(\vec{x}_\perp))$$

where
$$y_{\rm CM}(\vec{x}_\perp) = \text{arctanh}\left[\frac{T_A - T_B}{T_A + T_B}\tanh(y_{\rm beam})\right]$$

MUSIC [1] hydro with Lattice EoS [2]

T_A , T_B are nuclear thickness functions at $x_\perp$
- smooth or e-by-e fluctuating [3]

[1] PRC102 (2020) 014909
[2] PRC82 (2010) 014903
[3] PRC102 (2020) 044905

Similar reasoning as in this case…

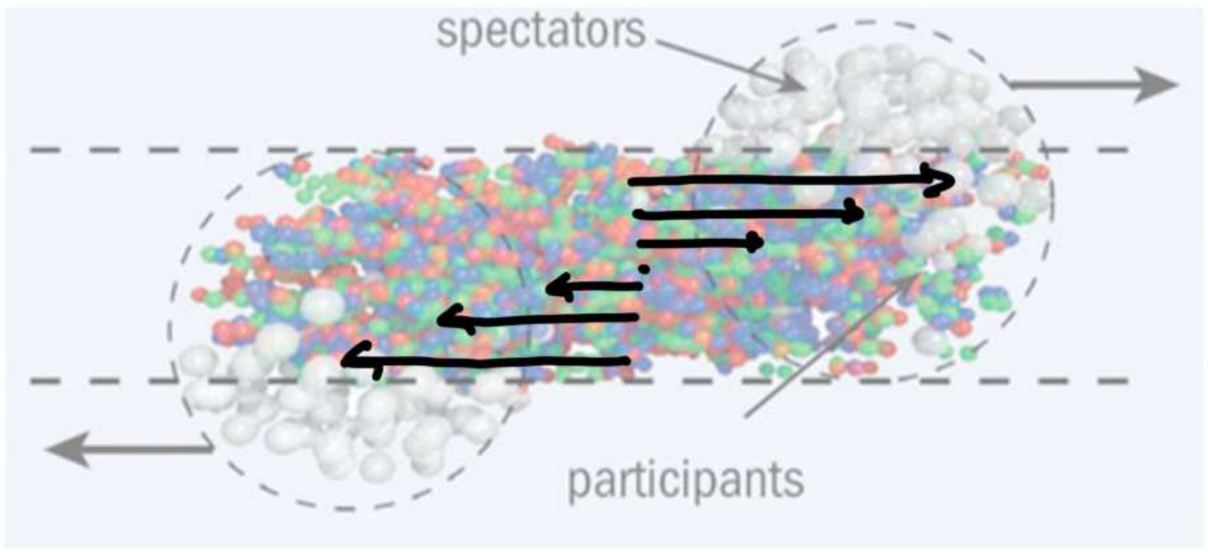

f=1

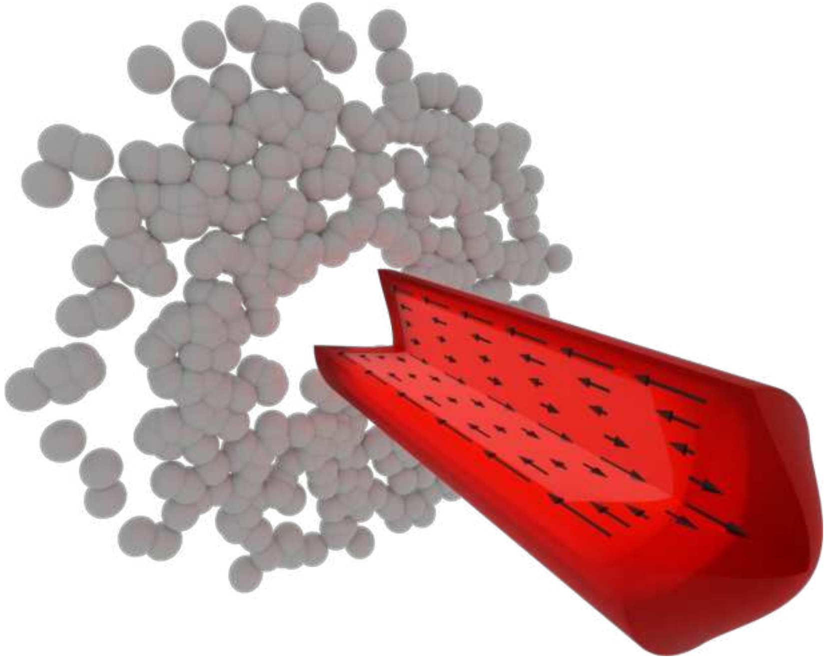

(b) Matter-overlap flow profile

Initial state

- Basic observables are ~identical in these scenarios

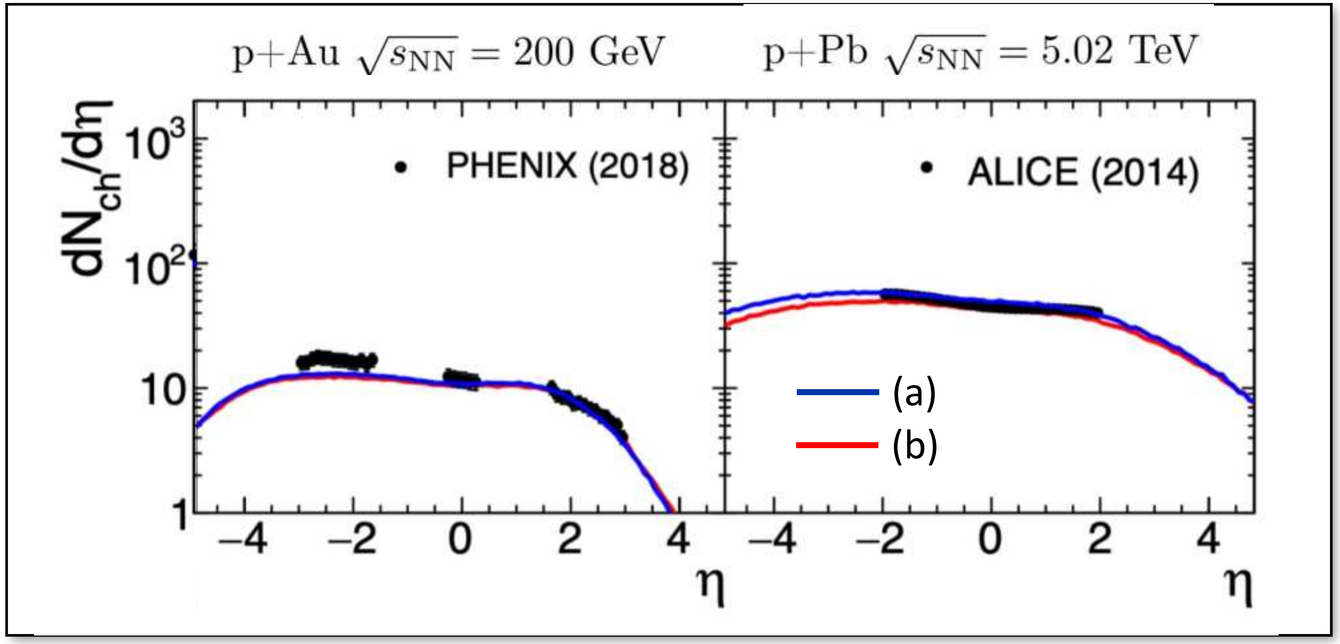

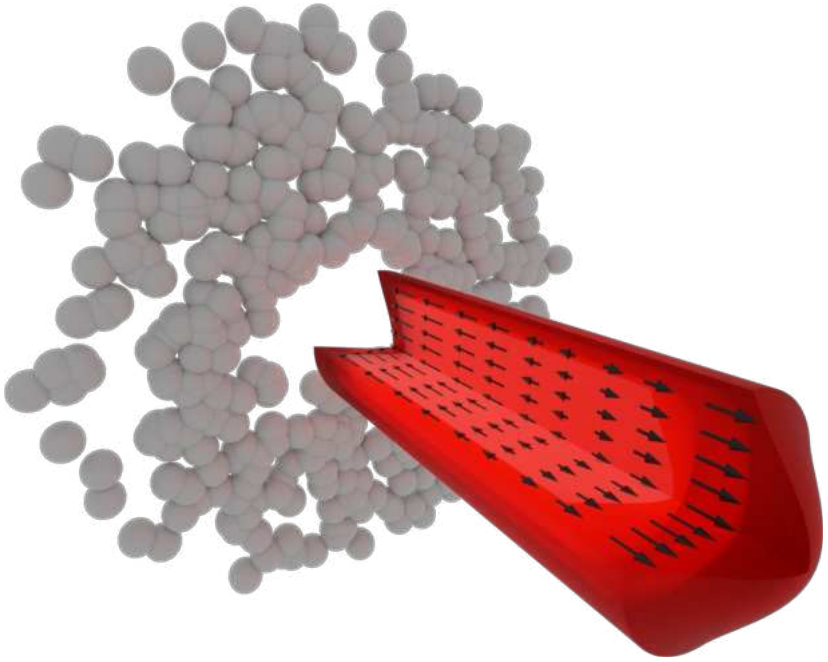

(a) Bjorken flow profile: $u_z = \eta_s$

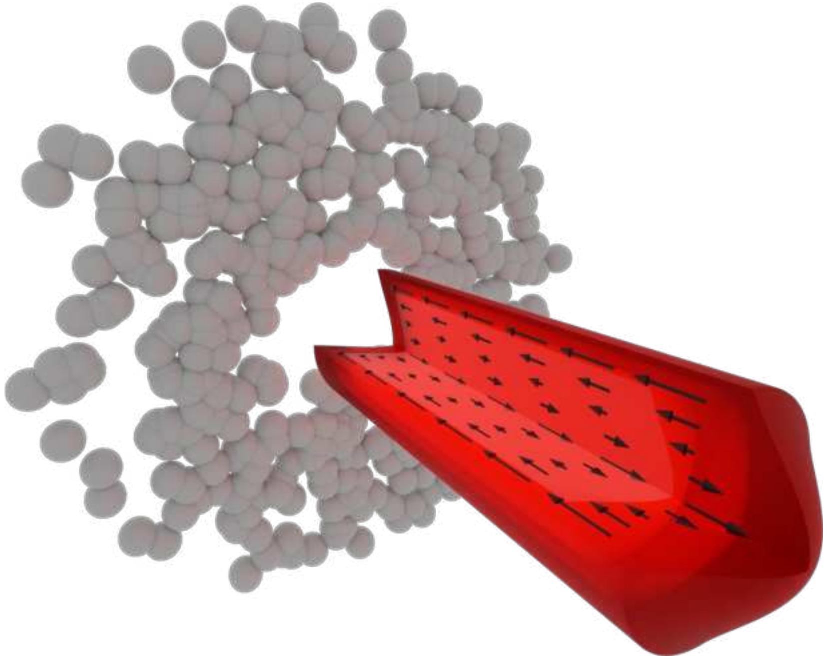

(b) Matter-overlap flow profile

Initial state

- Basic observables are ~identical in these scenarios
- **Vorticity is very different**

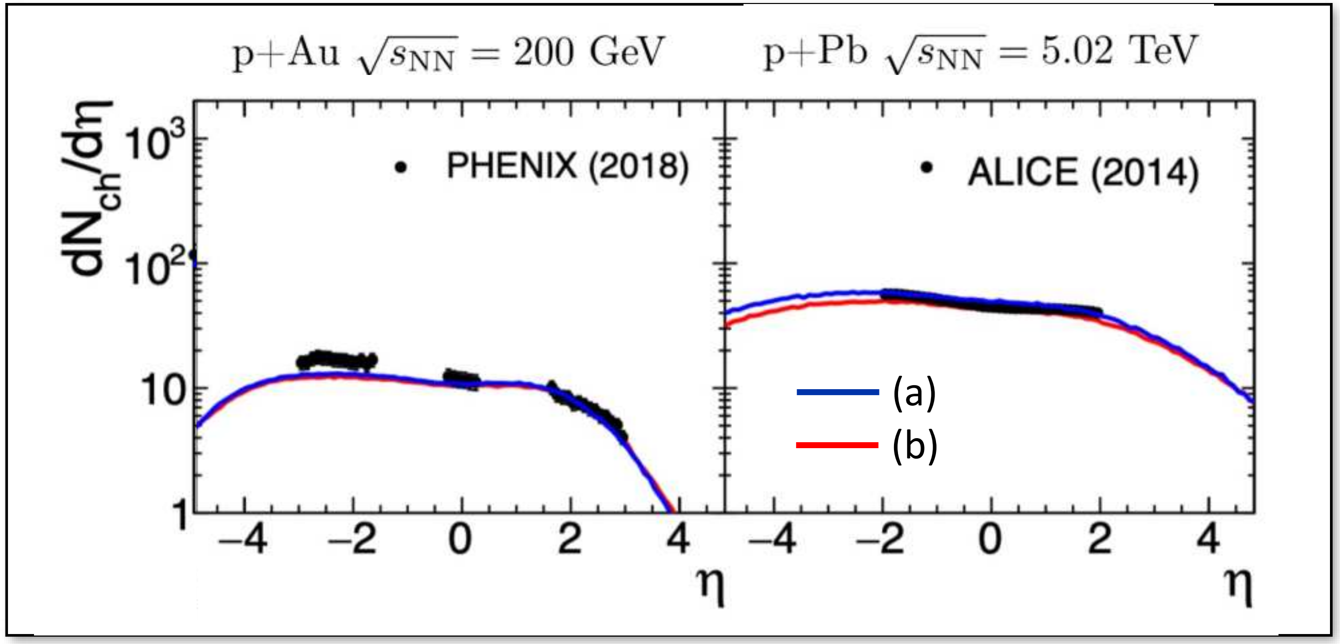

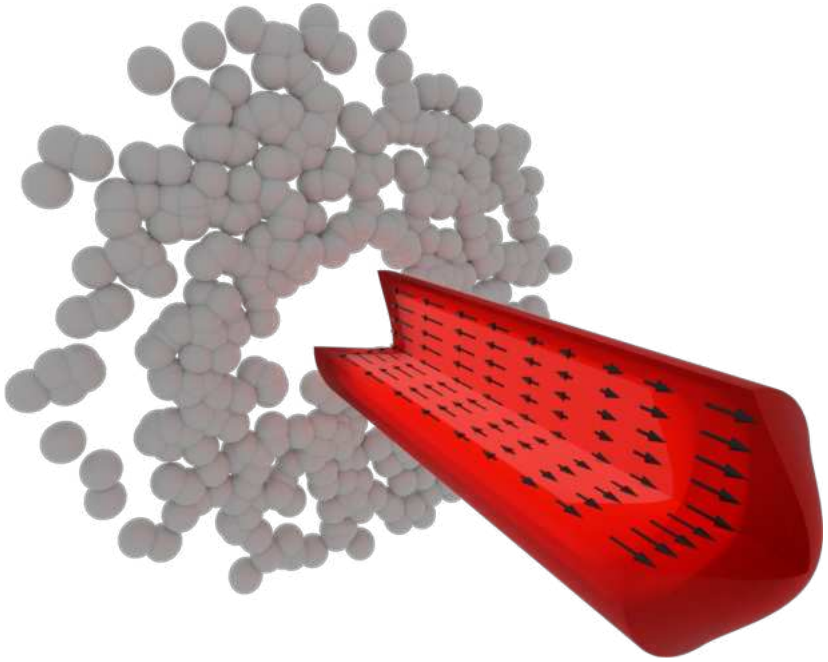

(a) Bjorken flow profile: $u_z = \eta_s$

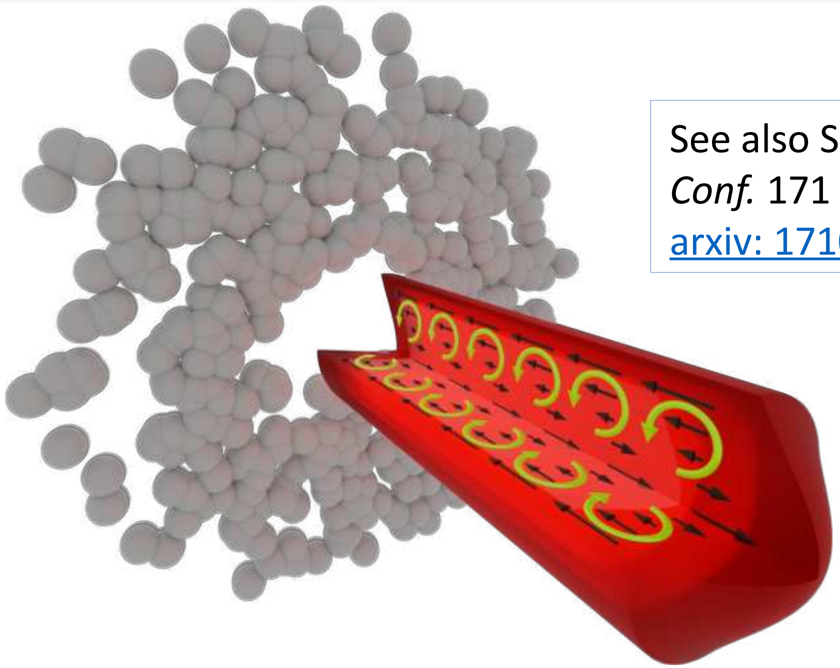

(b) Matter-overlap flow profile

See also S. Voloshin, *EPJ Web Conf.* 171 (2018) 07002
[arxiv: 1710.08934]

PR**C104** (2021) 1, 011901

Initial state

- Basic observables are ~identical in these scenarios
- **Vorticity is very different**

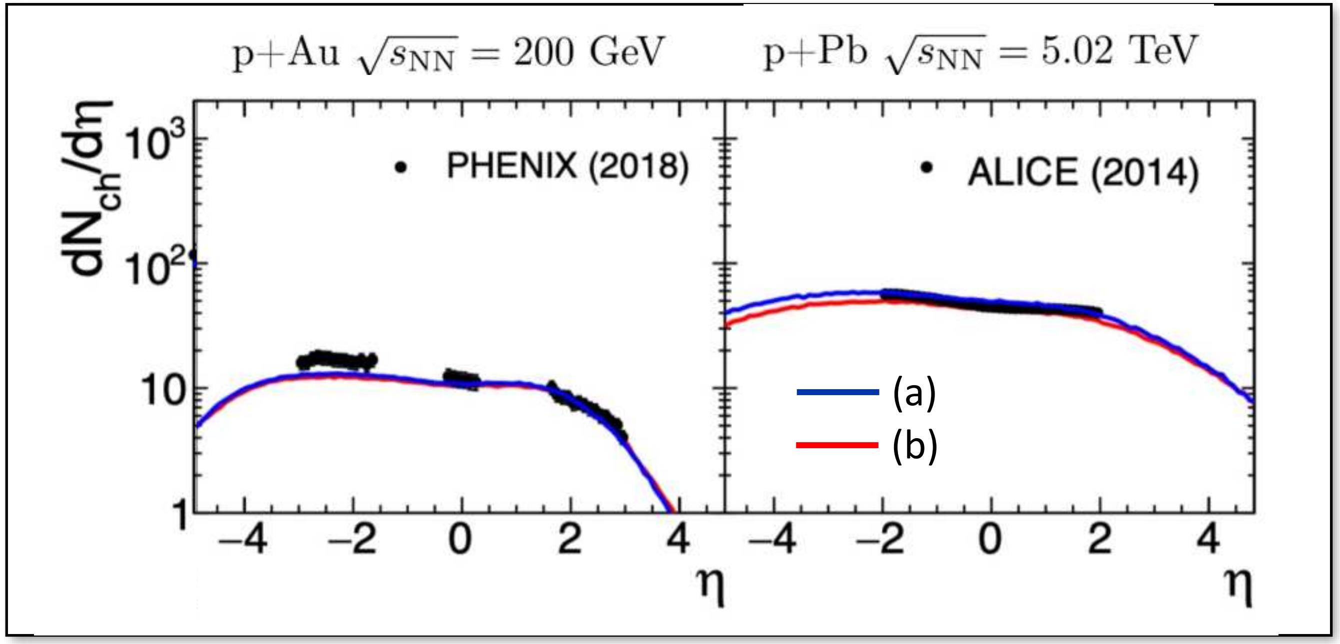

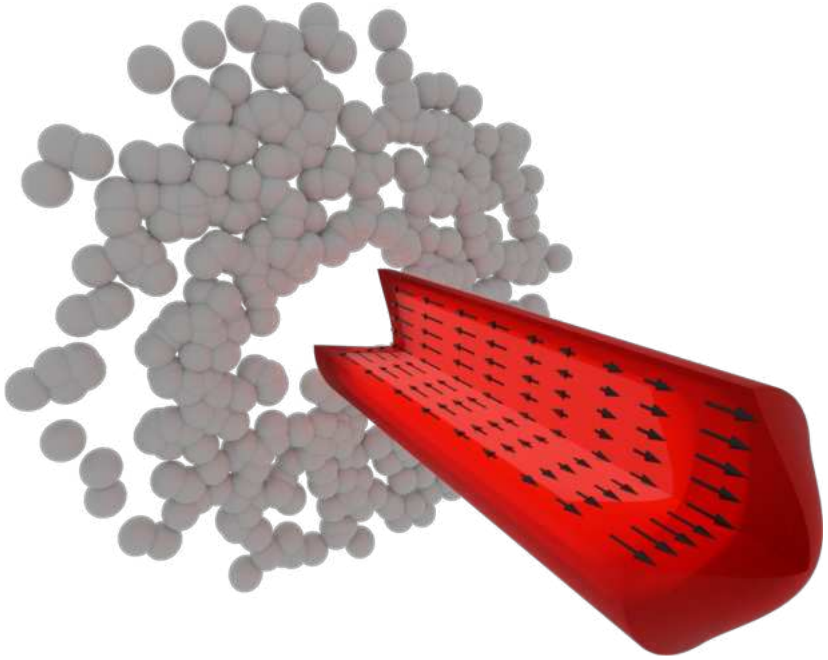

(a) Bjorken flow profile: $u_z = \eta_s$

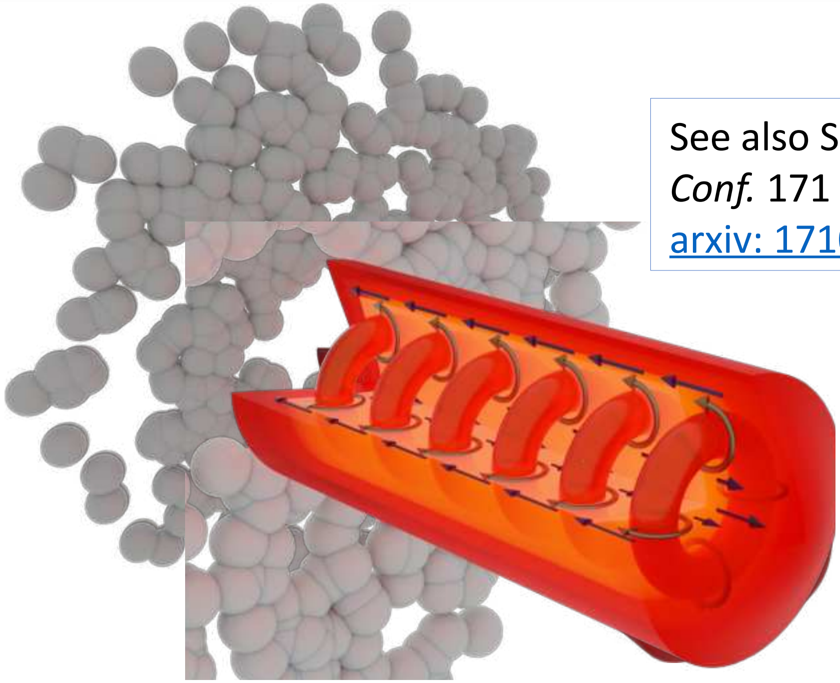

See also S. Voloshin, *EPJ Web Conf.* 171 (2018) 07002
arxiv: 1710.08934

(b) Matter-overlap flow profile

PR**C104** (2021) 1, 011901

Relation to Takahashi geometry

The experimental geometry was **not** this

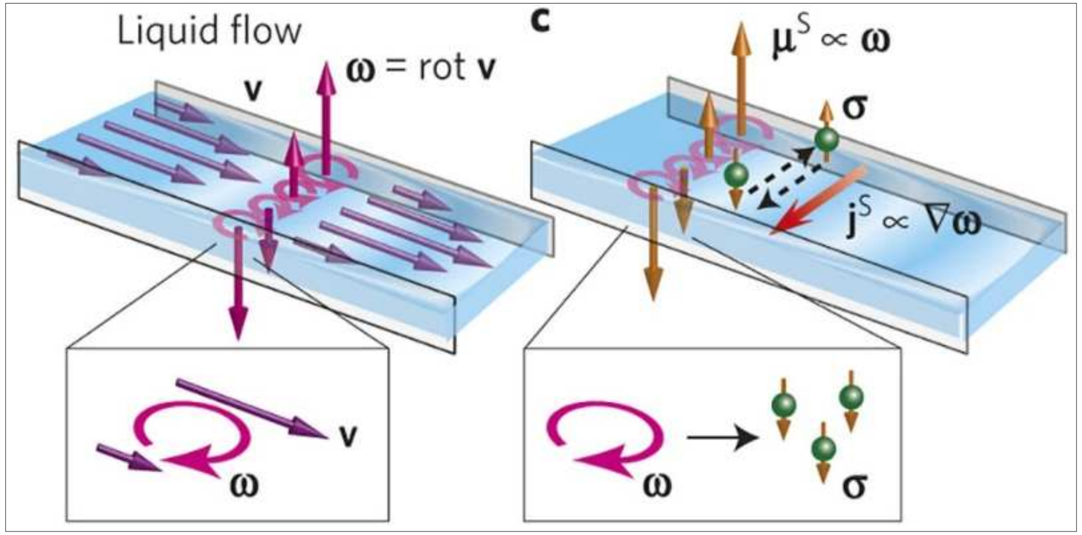

R. Takahashi, Nature Phys. 12 (2016) 52-56

It was flow thru capillary tube:

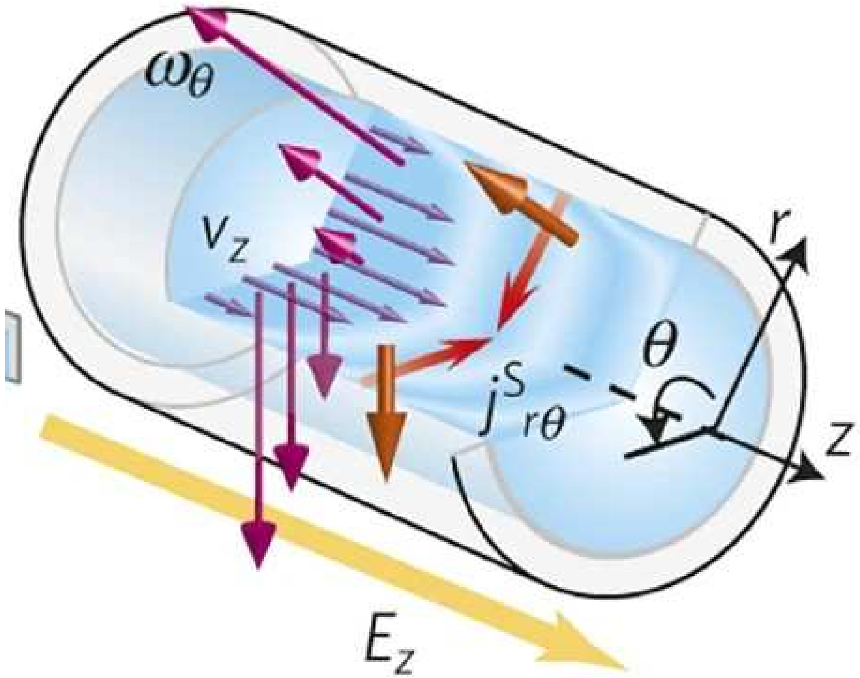

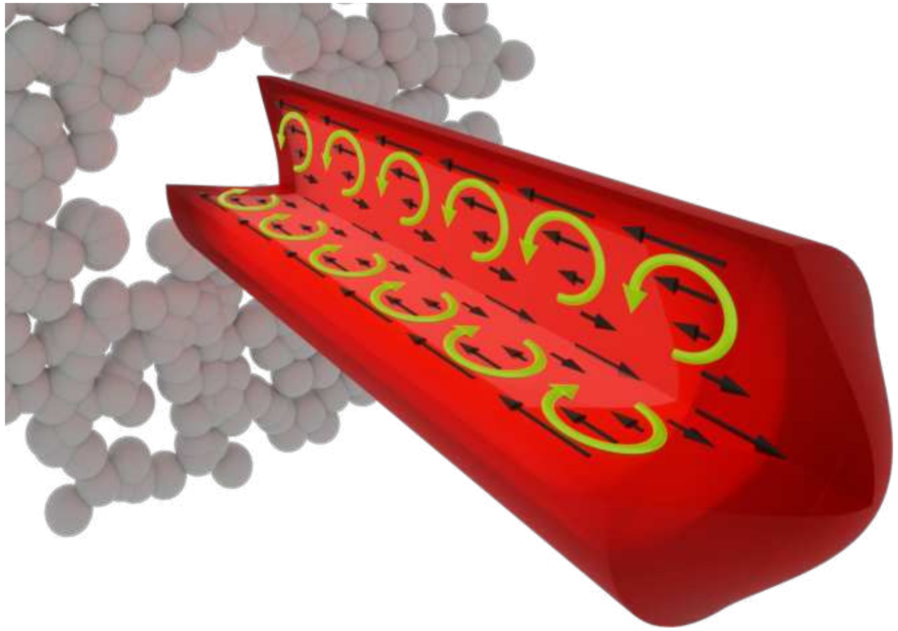

(b) Radial-gradient flow profile

PR**C104** (2021) 1, 011901

color axis: $\overline{\mathcal{R}}^{\hat{t}}_{\rm NR} \equiv \left\langle \frac{\vec{\omega}_{\rm NR} \cdot (\hat{t} \times \vec{v}_{\rm cell})}{|\hat{t} \times \vec{v}_{\rm cell}|} \right\rangle_\phi$ → $\mathcal{R}^{\hat{t}}_{\rm fluid} \equiv \frac{\epsilon^{\mu\nu\rho\sigma}\Omega_\mu n_\nu \hat{t}_\rho u_\sigma}{|\epsilon^{\mu\nu\rho\sigma} n_\nu \hat{t}_\rho u_\sigma|}$ | → $\vec{\omega}$ (red) | → $\vec{u}_{\rm cell}$ (green)

p+Au at 200 GeV

(a)

(b)

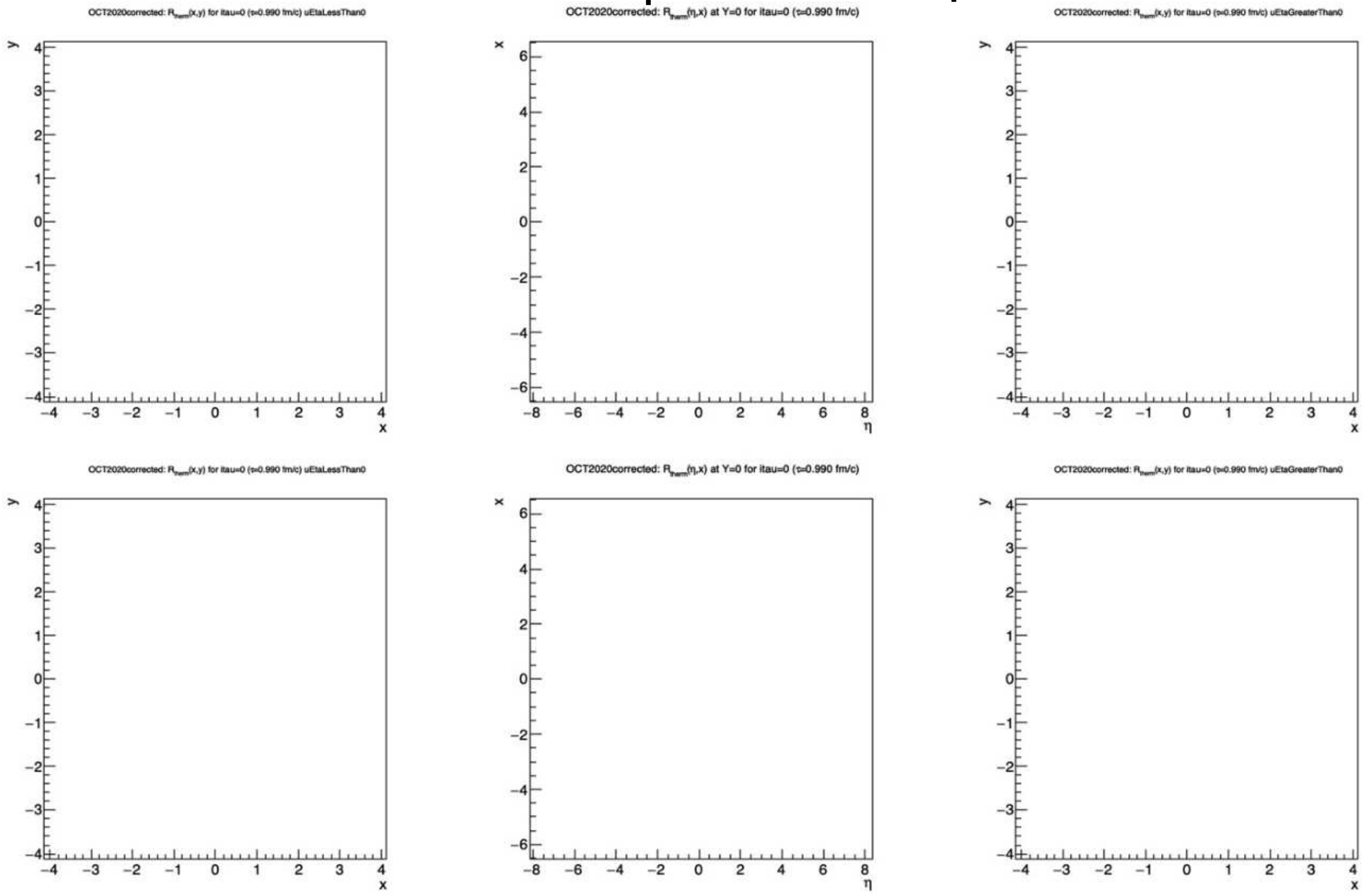

MUSIC hydrodynamics, with baryon currents

PRC**104** (2021) 1, 011901

PRC104 (2021) 011901; arxiv: 2101.10872

Snaphots

Au+Au

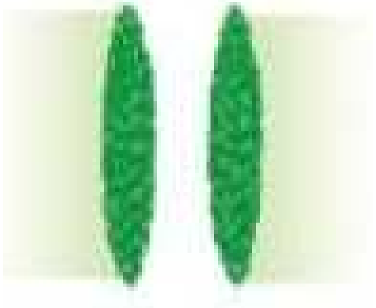

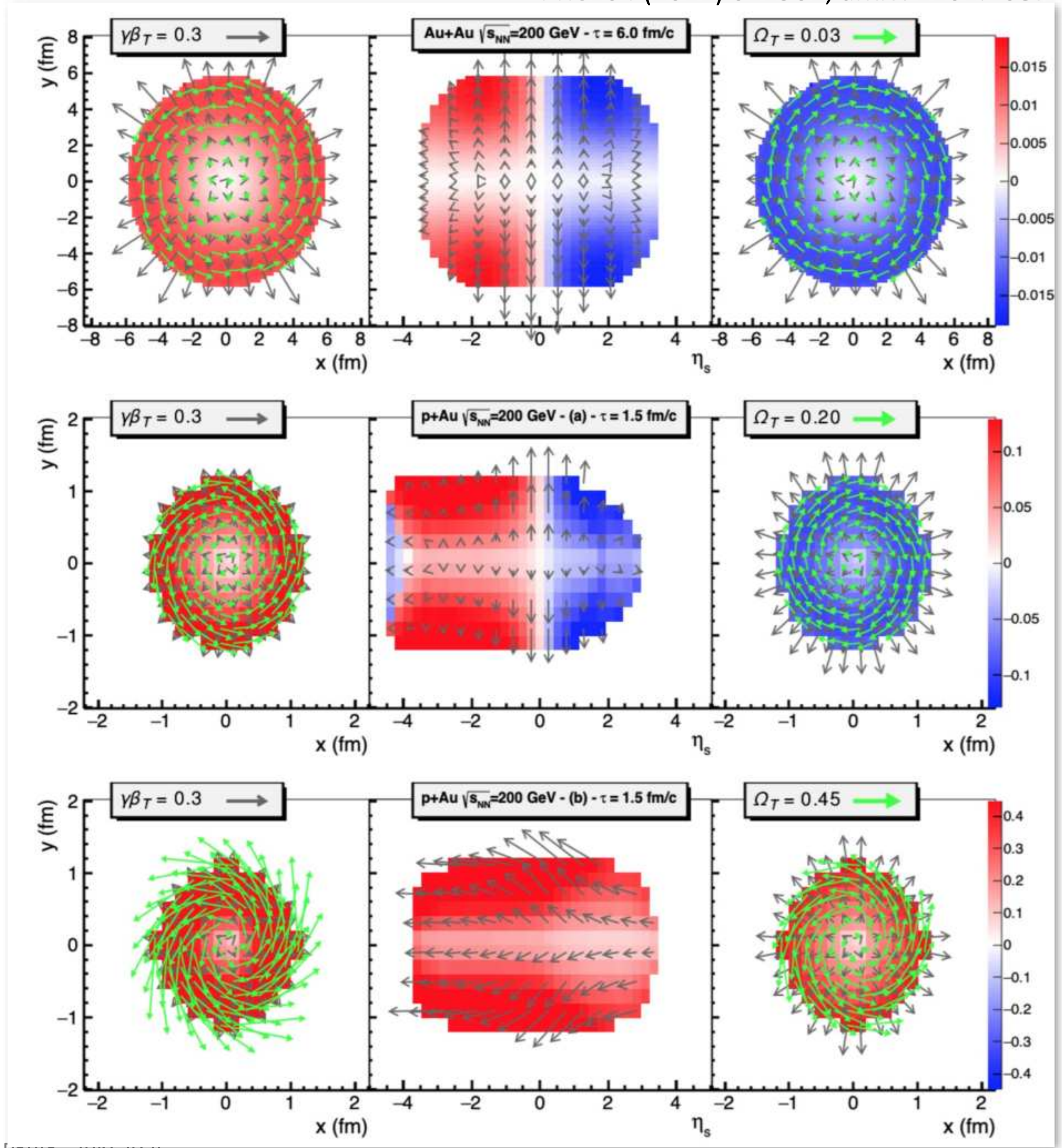

p+Au bjorken flow
- similar Au+Au

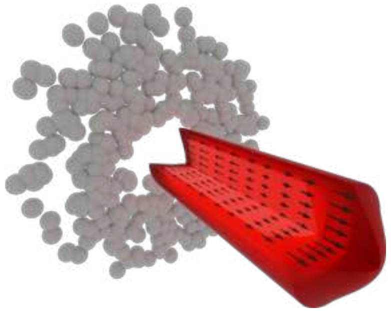

p+Au matter-overlap flow
- strong
- ~rapidity-even

smooth-on-smooth, b=0 collisions at 200 GeV

Fluid → particles (vorticity → polarization)

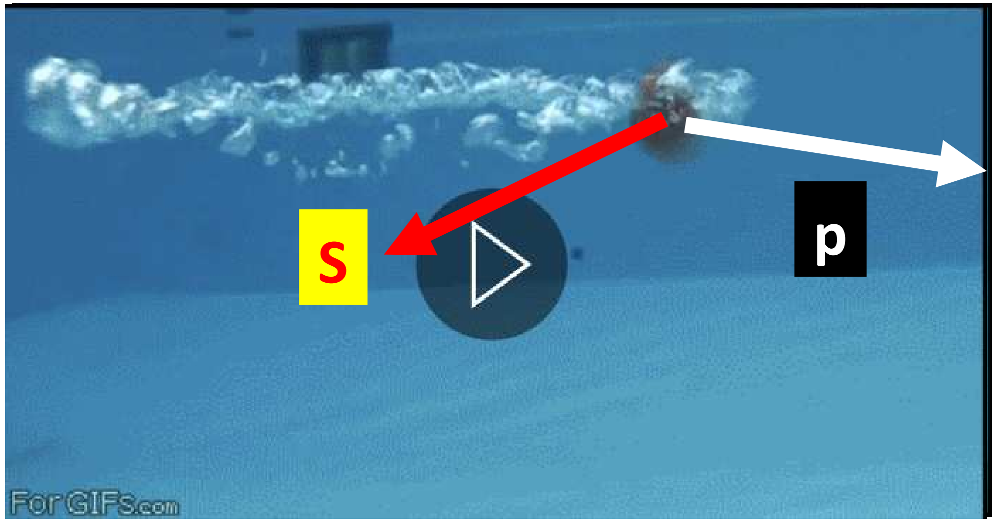

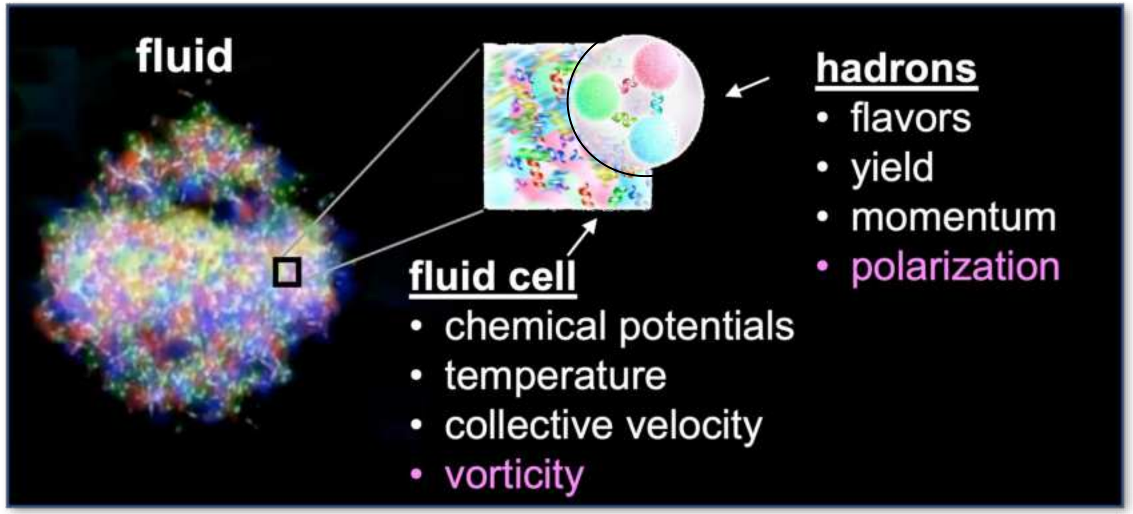

Cooper-Frye for spin

$$S^\mu(p) = -\frac{1}{8m}\epsilon^{\mu\rho\sigma\tau}p_\tau \frac{\int d\Sigma_\lambda p^\lambda n_F(1-n_F)\omega_{\rho\sigma}}{\int d\Sigma_\lambda p^\lambda n_F}$$

Becattini et al, Annal. Phys. 338 (2013) 32

$$\omega^{(th)}_{\mu\nu} = -\tfrac{1}{2}\left[\partial_\mu\left(u_\nu/T\right) - \partial_\nu\left(u_\mu/T\right)\right]$$

(or alternative vorticities…)

$$\omega^{(K)}_{\mu\nu} = -\tfrac{1}{2}\left(\partial_\mu u_\nu - \partial_\nu u_\mu\right)$$

$$\omega^{(T)}_{\mu\nu} = -\tfrac{1}{2}\left[\partial_\mu\left(T u_\nu\right) - \partial_\nu\left(T u_\mu\right)\right]$$

non-vortical symmetric shear

$$\xi^{\mu\nu} \equiv \frac{1}{2}\left[\partial^\mu\left(\frac{u^\nu}{T}\right) + \partial^\nu\left(\frac{u^\mu}{T}\right)\right]$$

$$S_\mu \rightarrow S_\mu + \langle \mathcal{A}_\mu \rangle$$

$$\mathcal{A}_\mu = \frac{1}{E}\epsilon^{\mu\rho\tau\sigma}p_\tau \xi_{\sigma\lambda} \times \begin{cases} \hat{t}_\rho p^\lambda & \leftarrow \text{Becattini et al (2021)} \\ u_\rho p^\lambda_\perp & \leftarrow \text{Liu \& Yin (2001)} \end{cases}$$

Observing the "smoke tubes"

Ring vorticity observable

$$\overline{\mathcal{R}}_{\Lambda}^{\hat{z}} = 2\left\langle \frac{\vec{S}'_{\Lambda}\cdot(\hat{z}'\times\vec{p}_{\Lambda}')}{|\hat{z}'\times\vec{p}_{\Lambda}'|} \right\rangle_{\phi}$$

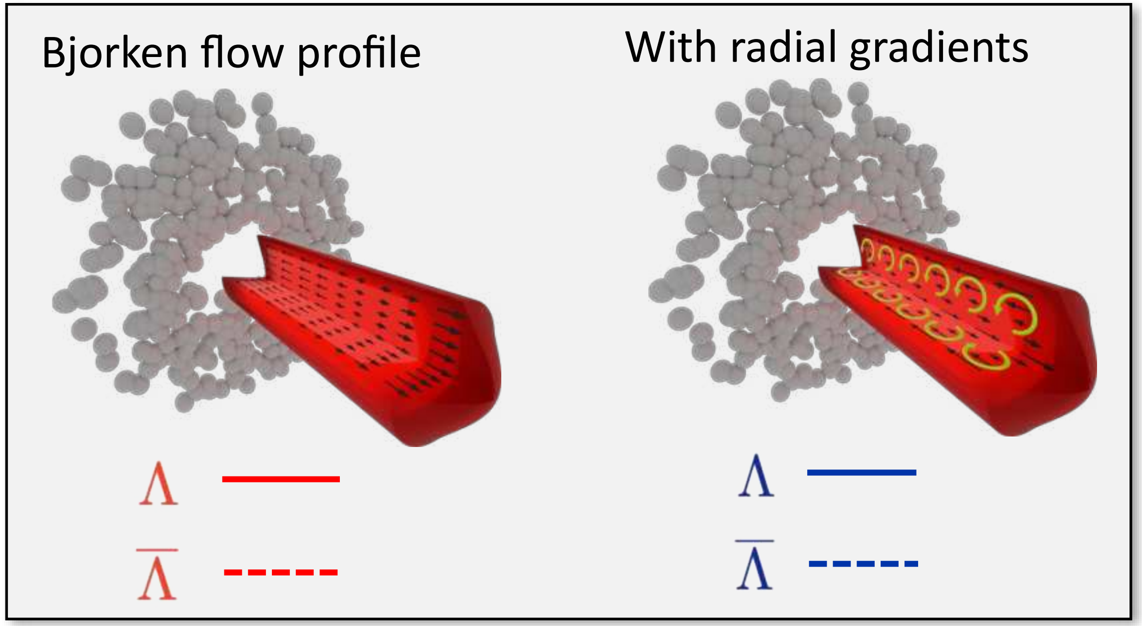

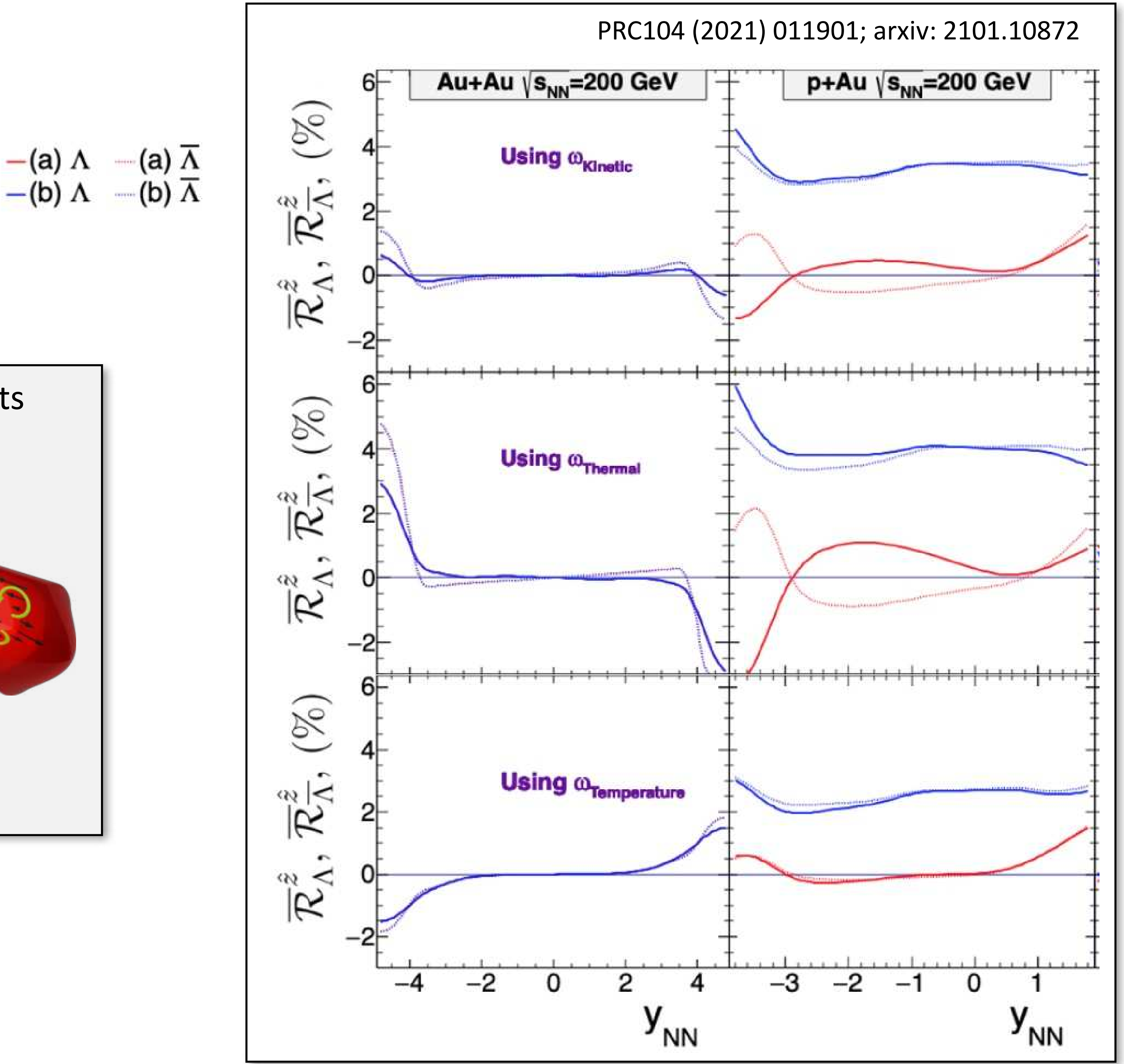

- similar effect for all vorticity "flavors"
- **hyperon and anti-hyperon are similar**

fluctuating initial conditions

PRC110 (2024) 054908

- ✓ Event-by-event calculation with lumpy initial conditions, following prescription in [1]
  → little difference with smooth initial conditions
- ✓ reduced R_{spin} for more symmetric system

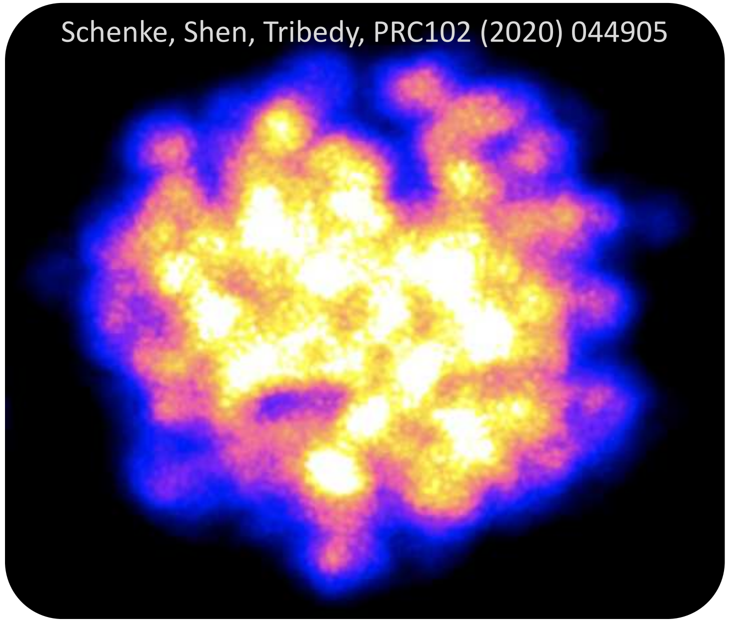

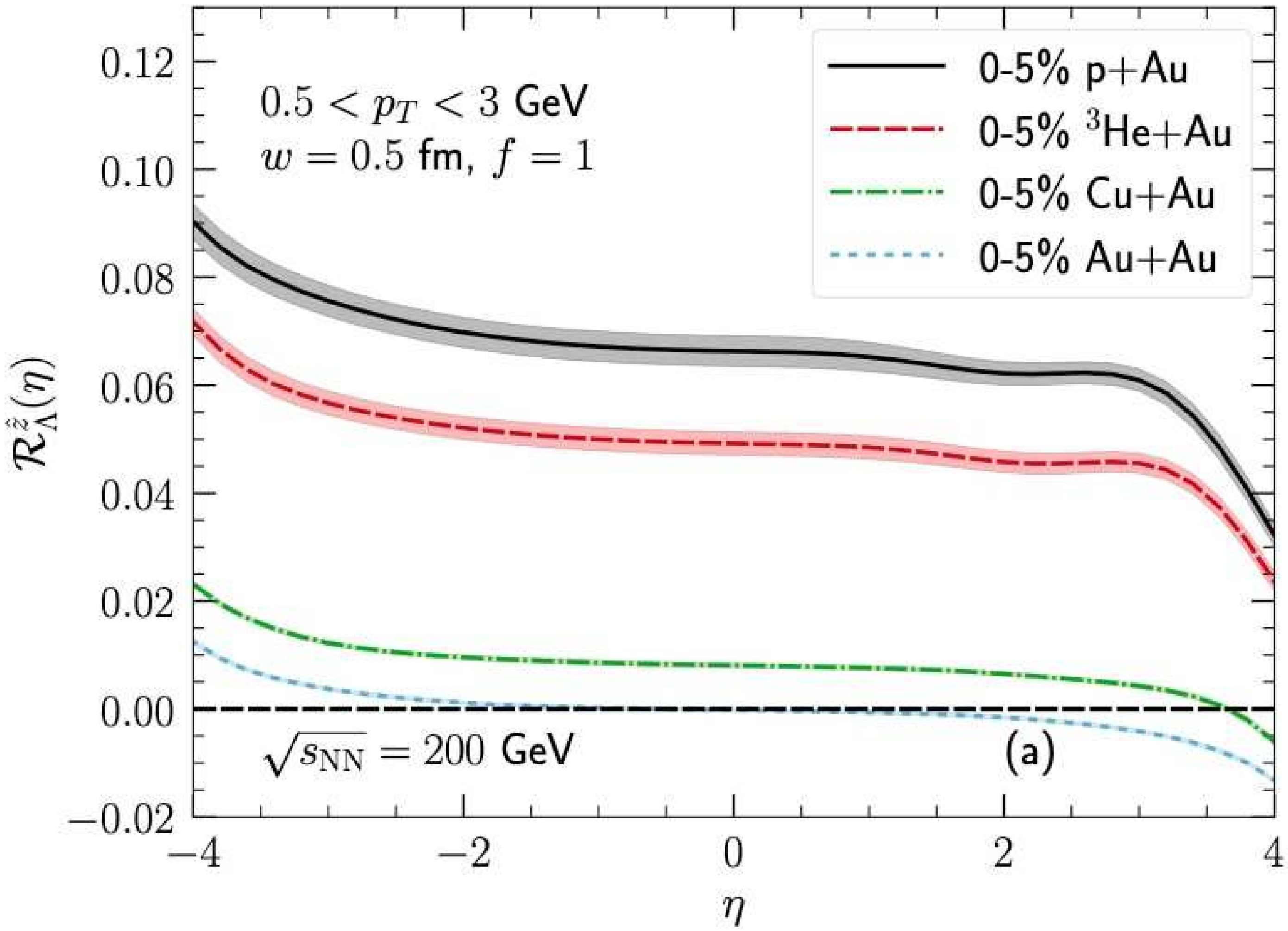

[1] Shen, Alzhrani, PRC102 (2020) 014909

Vortex rings at top RHIC energy: momentum dependence

PRC110 (2024) 054908

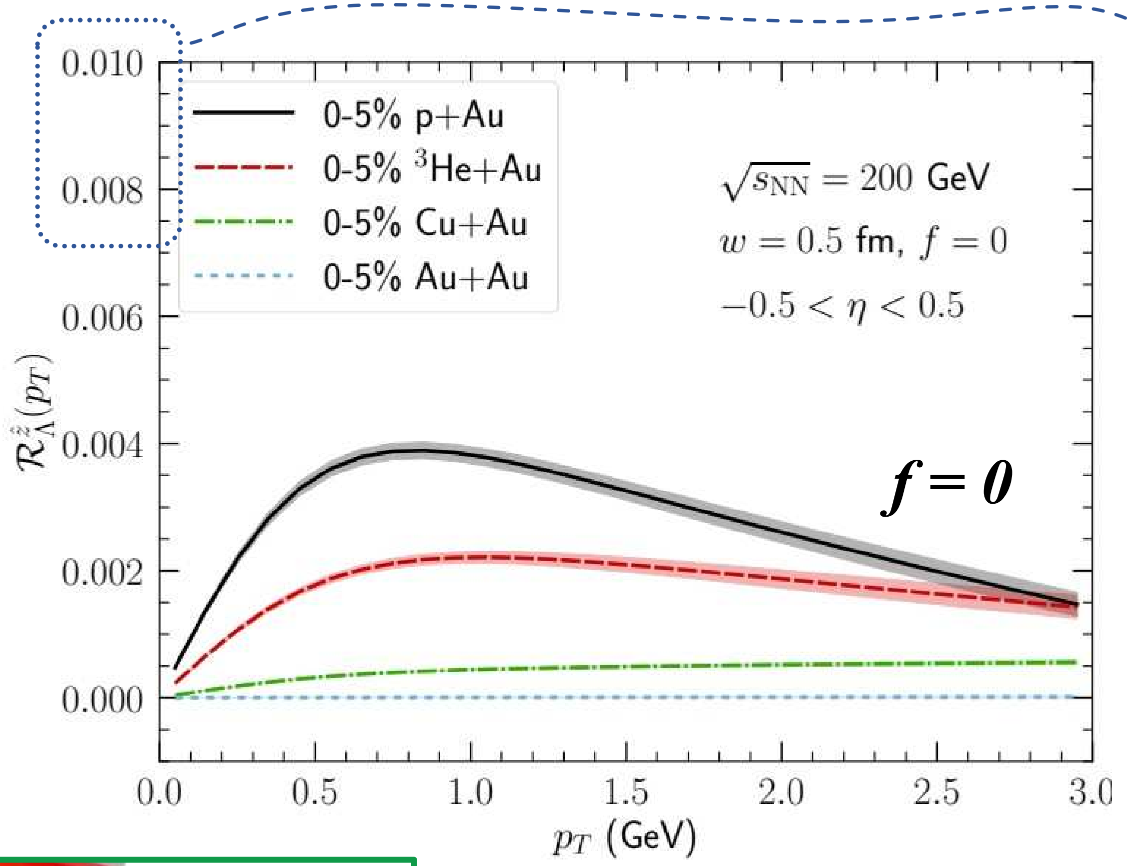

10x !

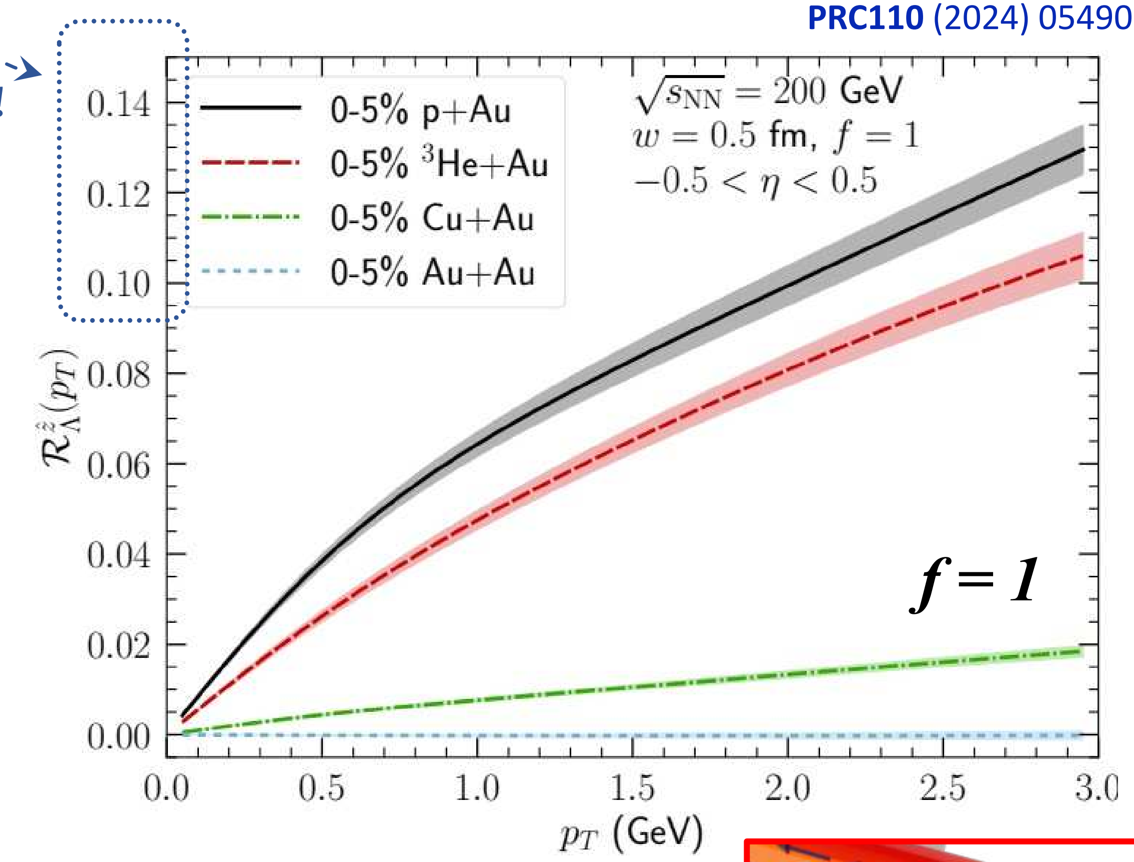

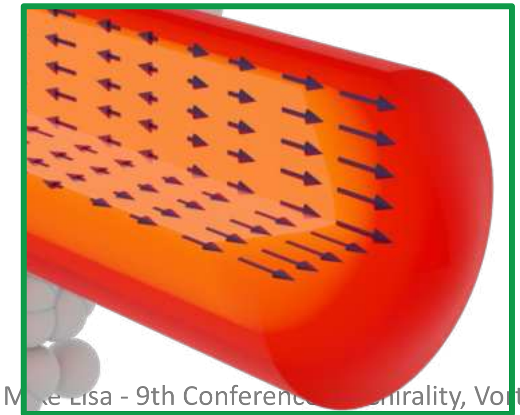

Much larger and qualitatively different pT dependence with $x_\perp$-dependent longitudinal flow

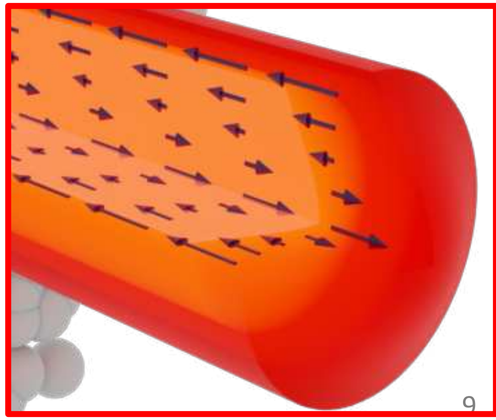

LHCb SMOG: predictions for the LHC

PRC110 (2024) 054908

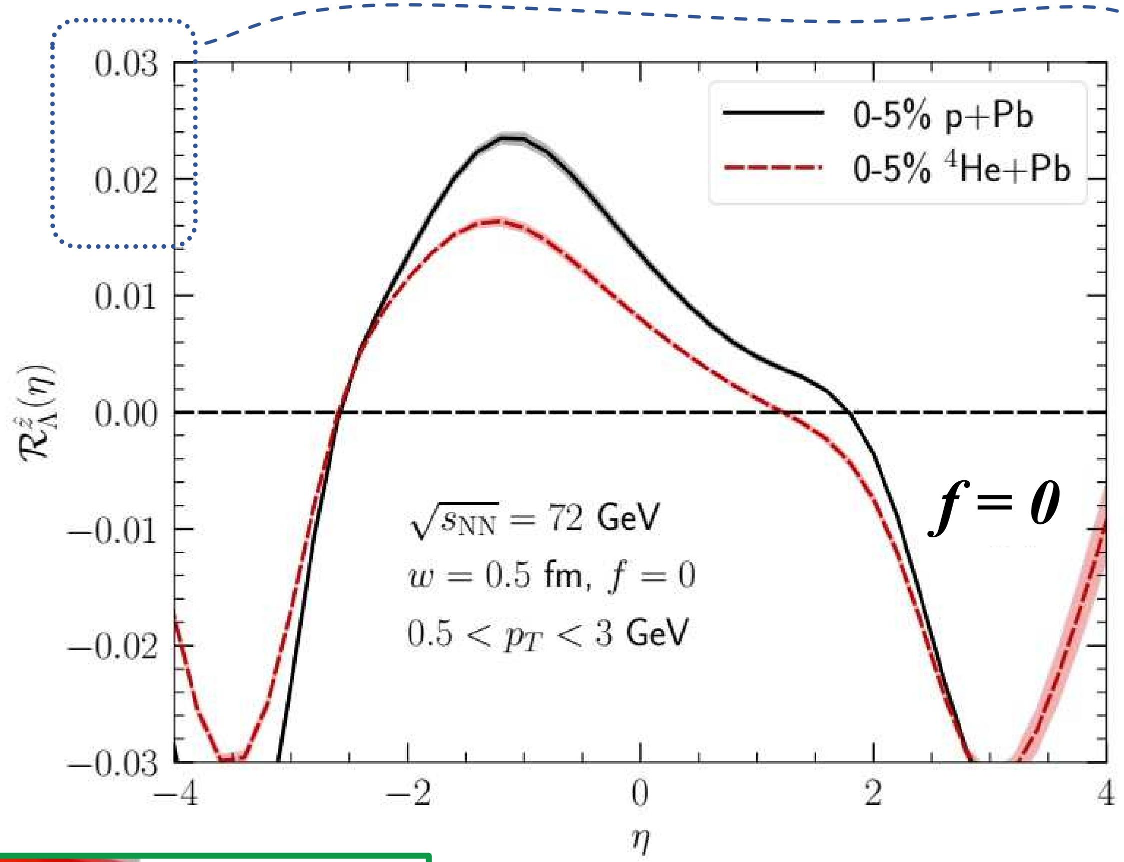

10x !

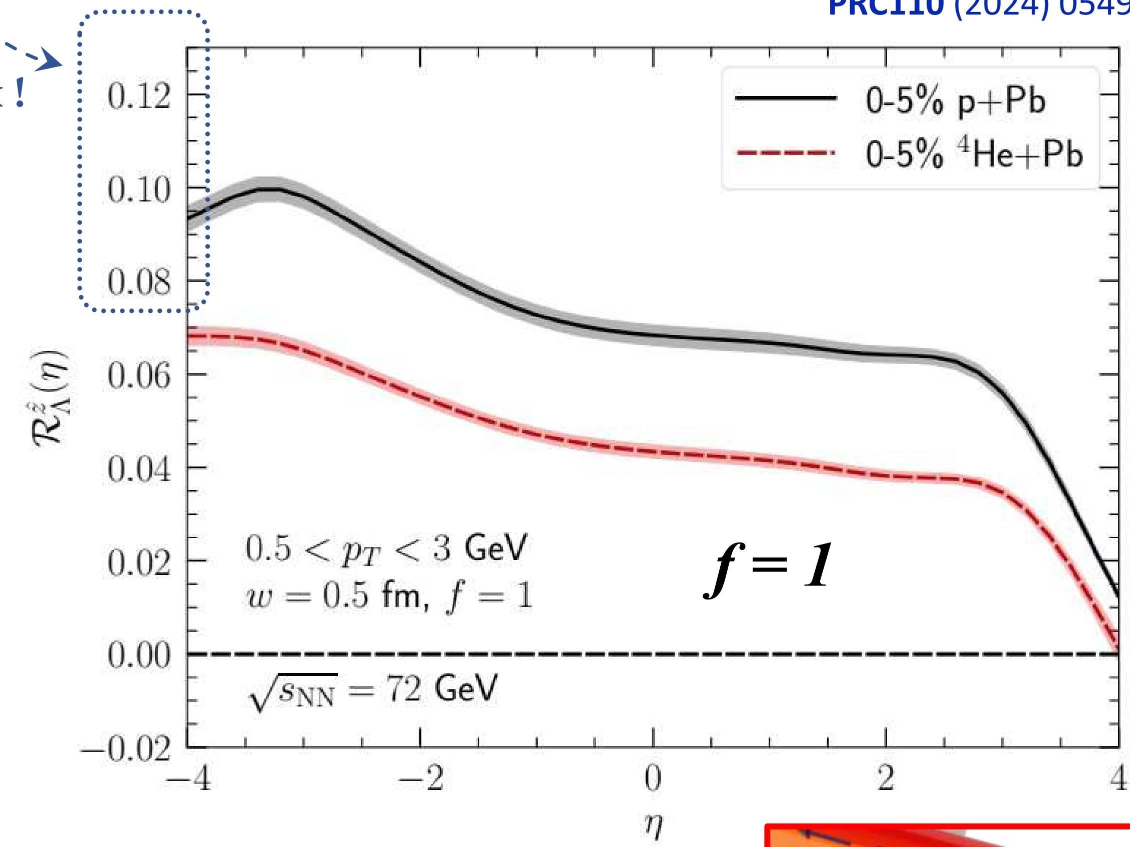

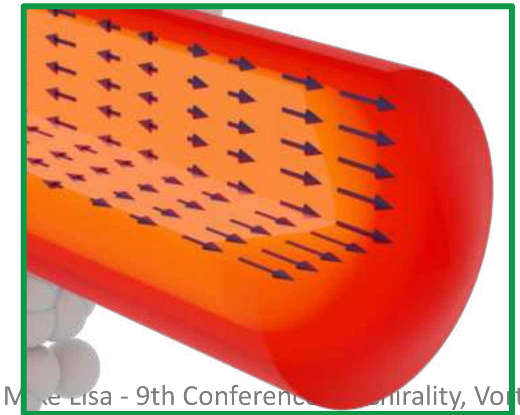

Fixed-target p-A runs at LHCb

- wide eta reach
- similar signal to RHIC

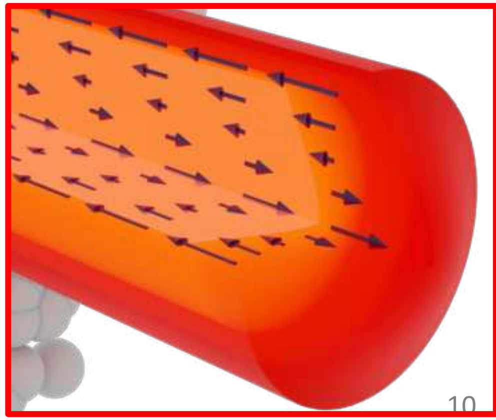

Sensitivity to physics of “smallest droplet of QGP”

PR110 (2024) 054908

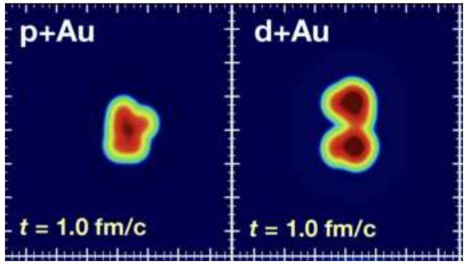

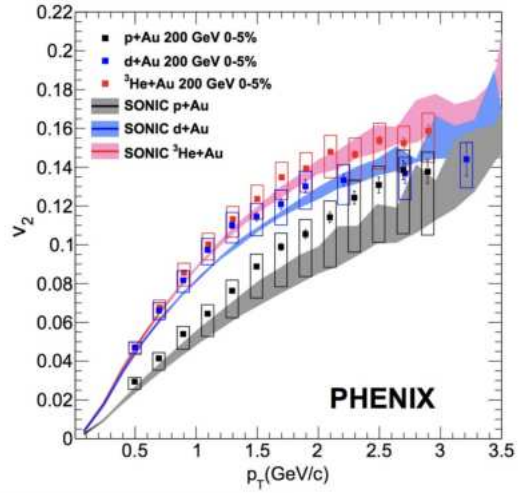

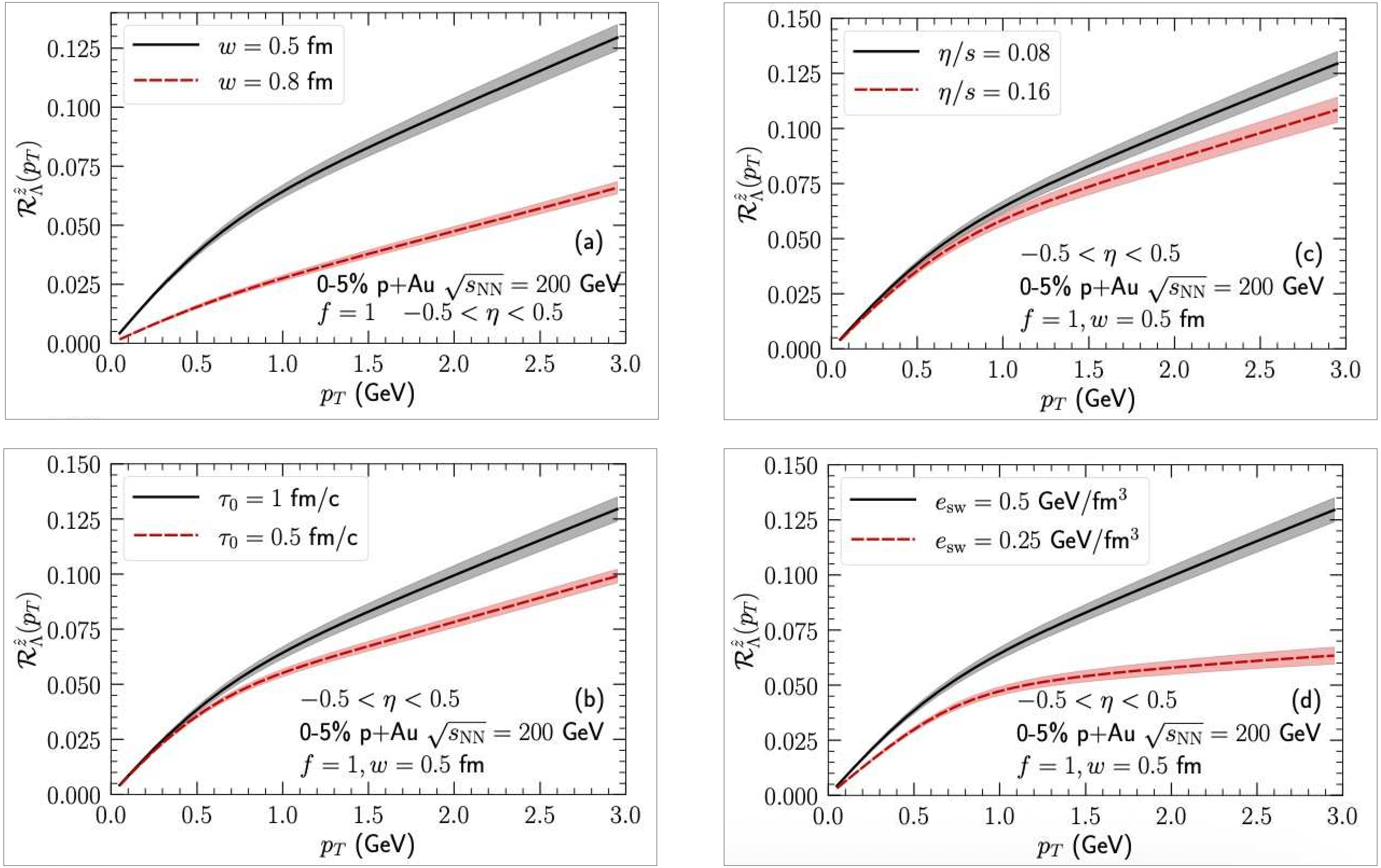

Sensitive to physics
- droplet size
- η/s
- τ_{therm}
- ε_{FO}

Experimental issues

$$\overline{\mathcal{R}}_{\Lambda}^{\hat{z}} = 2\left\langle \frac{\vec{S}_{\Lambda}'\cdot\left(\hat{z}'\times\vec{p}_{\Lambda}'\right)}{\left|\hat{z}'\times\vec{p}_{\Lambda}'\right|} \right\rangle_{\phi} = \frac{8}{\pi\alpha}\left\langle \sin\left(\phi_p - \phi_{\Lambda}\right)\right\rangle$$

Advantage:

- no event plane needed!

  → measuring ~1% toroidal polarization is much easier than 1% global polarization (for same stats)

$$\overline{P}_H = -\frac{8}{\pi\alpha R_{\mathrm{EP}}^{(1)}}\left\langle \sin\left(\phi_p - \Phi_{EP,1}\right)\right\rangle_{\phi}$$

$$\delta_{\overline{P}_H} \propto (\#_{\Lambda})^{-1/2}\left(R_{\mathrm{EP}}^{(1)}\right)^{-1}$$

~2-3

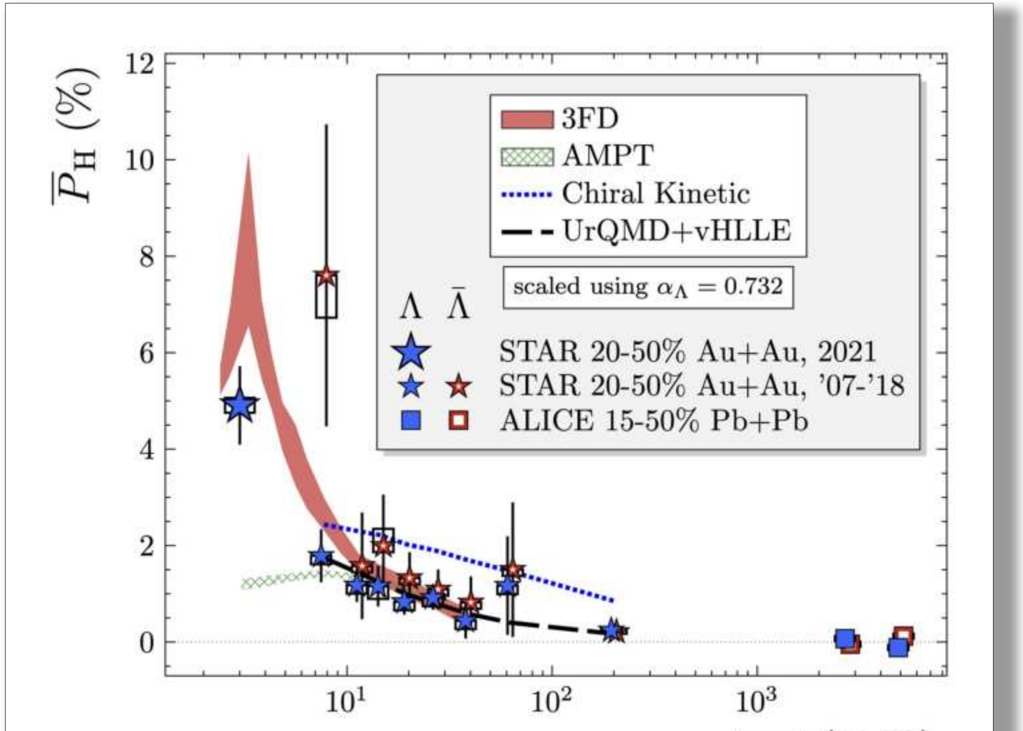

STAR PRC104 (2021) L061901

Required statistics:

- similar #Λ

  → scaling from 11 BES global polarization [1]: [300M central (0-10%) events]to discover 1% vortical polarization with 7σ significance

  ✓ 5-week p-Au run ~ 350 M

[1] STARNote **SN0819 : The STAR Beam Use Request for Run-24-25** https://drupal.star.bnl.gov/STAR/starnotes/public/SN0819

Crucial experimental issue

STARNote **SN0819 : The STAR Beam Use Request for Run-24-25**
https://drupal.star.bnl.gov/STAR/starnotes/public/SN0819

STAR data for
Au+Au $\sqrt{s_{NN}}$ = 27 GeV
from 2 different years

Note: physical signal zero by symmetry

- B-field points West
- original TPC
- hyperons found by topological cuts

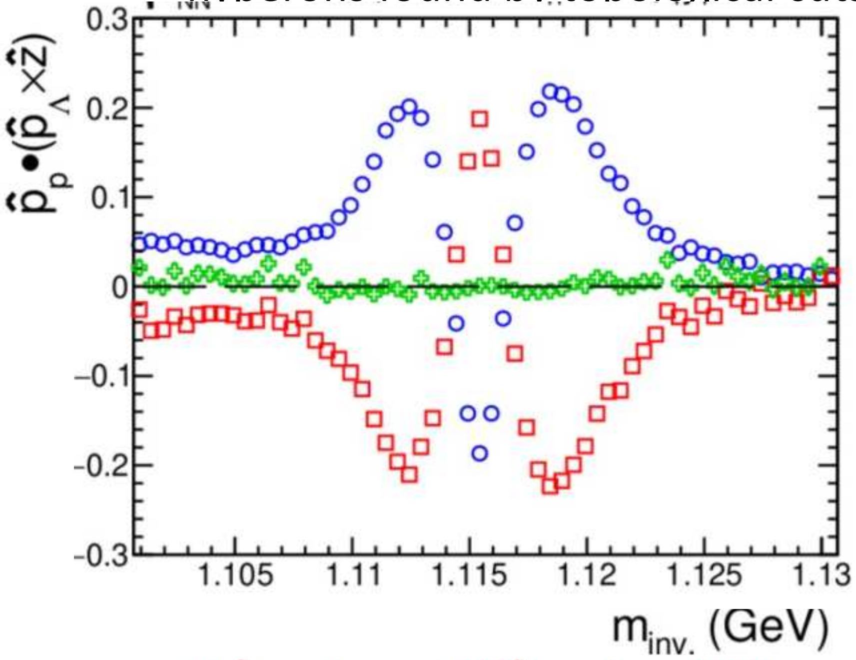

$\mathcal{R}_{\Lambda}^{\hat{z}} > 0$ and $\mathcal{R}_{\bar{\Lambda}}^{\hat{z}} > 0$???

- B-field points East
- upgraded TPC
- hyperons found by KFParticle

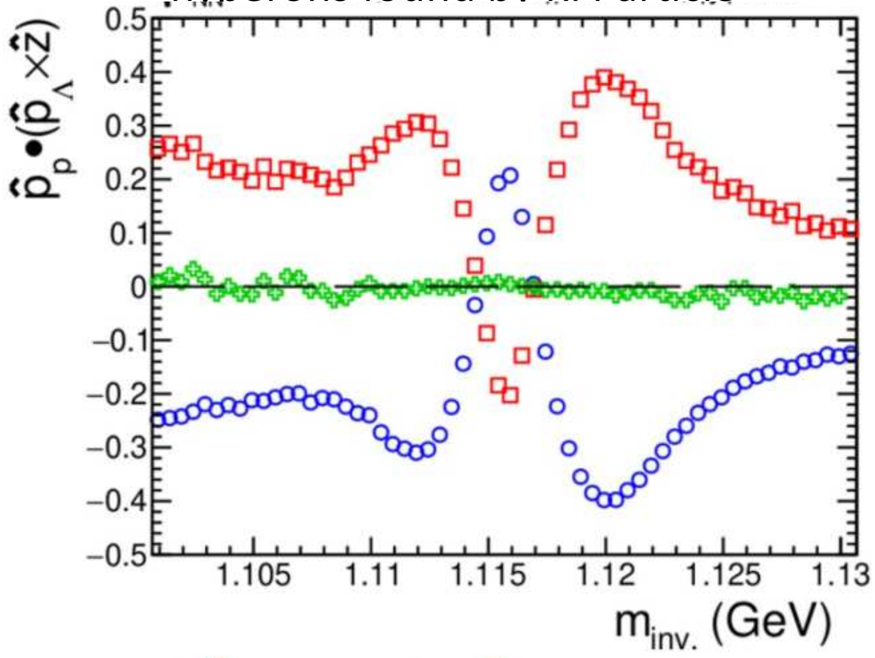

$\mathcal{R}_{\Lambda}^{\hat{z}} < 0$ and $\mathcal{R}_{\bar{\Lambda}}^{\hat{z}} < 0$???

- STAR: Midrapidity hyperons from Au+Au collisions – signal must vanish by symmetry
- Tracking-induced artifacts
  - **large**! – bigger than likely signal
  - **complicated**! – depends strongly on cuts, method, detector. Seen also in simulation, but not exactly the same
  - equal and opposite for Lambda & antiLambda → **artifact will flip with B-field**.

If STAR measures p+Au collisions in the final run, it must measure both field configurations!

Summary

- **A+A / p+A collisions generate complex flow structures; probed by vorticity at small scale**

- **Circular vorticity pattern predicted for b=0 collisions at all energies**
  - LHCb – take a look!

- **Fluid system with localized disturbance – toroidal vortex structure forms**
  - Helmholtz (1867): Persistent vortical toroids (smoke rings) are quintessential fluid behavior
  - thermalized energy from jet quenching – sensitive to virtuality, fluid properties
  - p+A - would be a compelling evidence for hydro nature of the smallest system & physical properties

- **Experimentally observable (*R*)**
  - distinct from hadronic processes by particle/antiparticle similarity, eta dependence
  - challenging to observe few % effect, but possible during this last RHIC run - flip B-field

Muito obrigado pela sua atenção

Backup

At very high $\sqrt{s_{NN}}$: signal reverses

Nontrivial dynamics for long lifetime

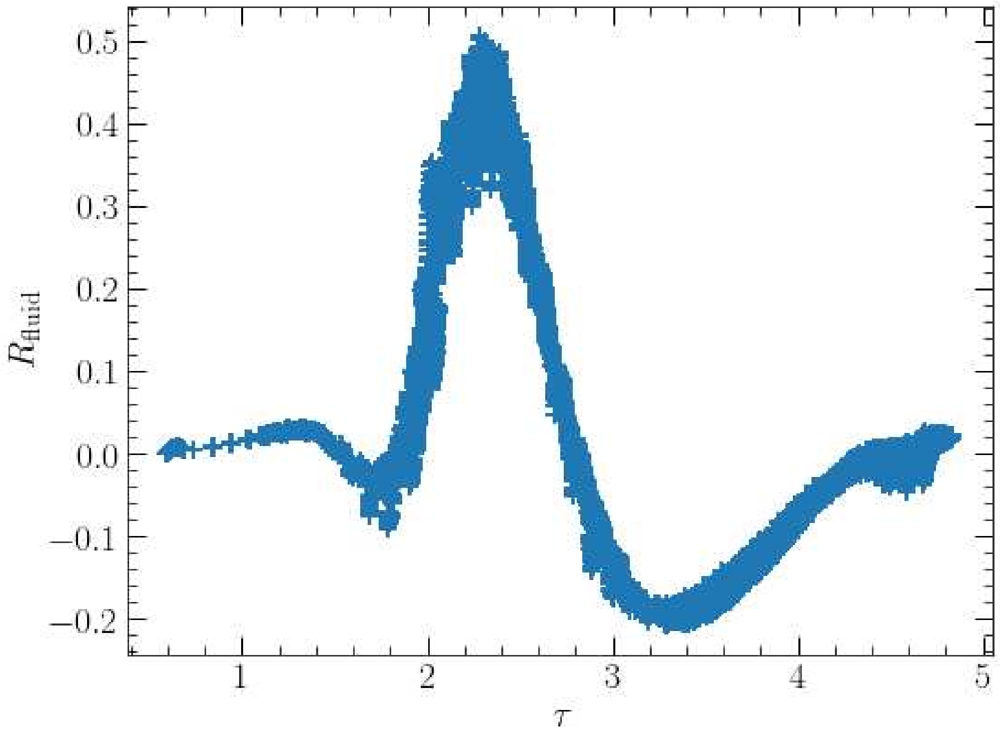

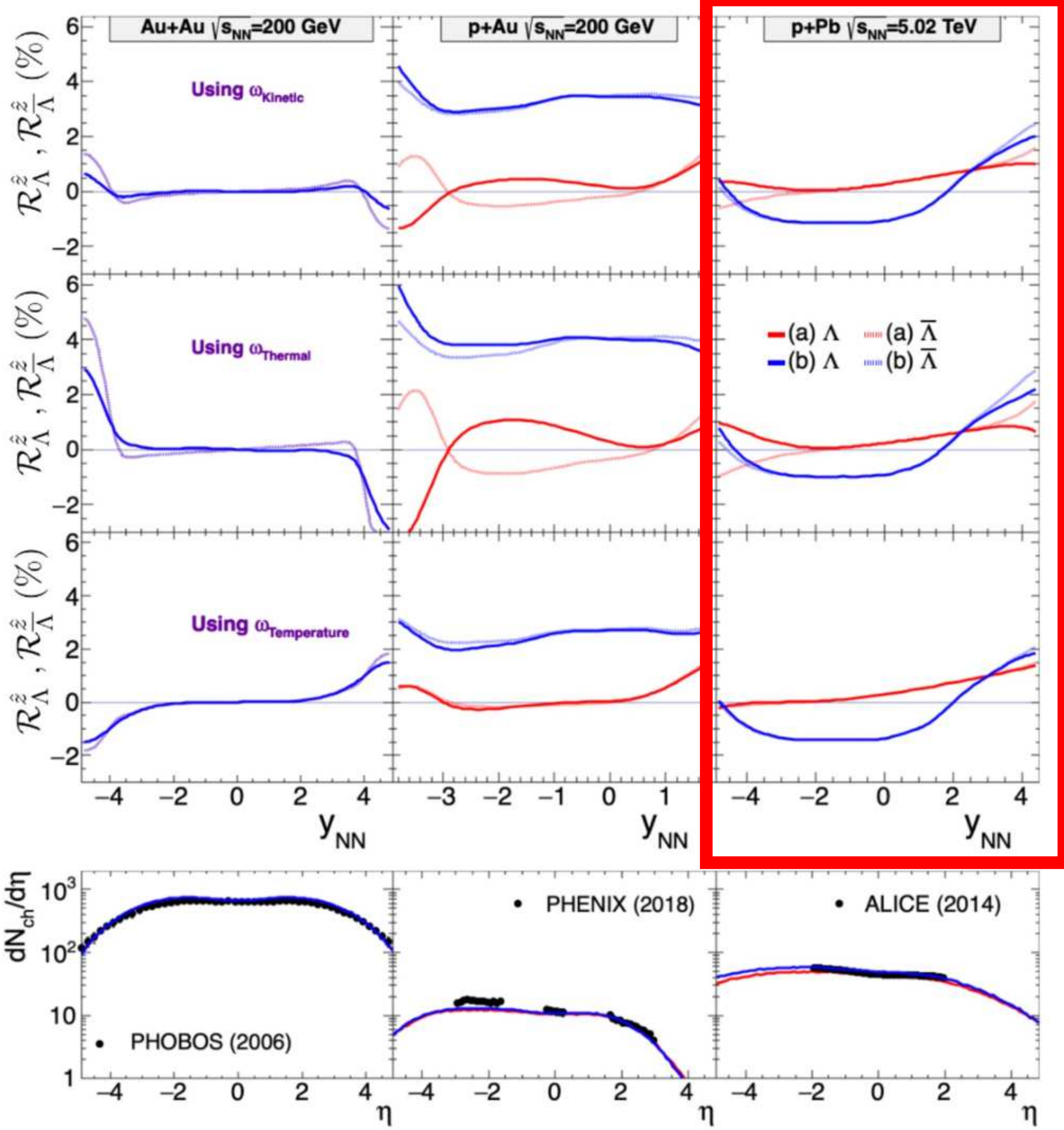

✓ RHIC energy is a good place to look

PRC104 (2021) 011901; arxiv: 2101.10872

Contributions from shear terms and gradients in chemical potential

- Formulation of Becattini et al has very strong effect
- Formulation of Liu et al significant at high pT
- Chemical gradients minor effect

$$S^{\mu}_{\mathrm{SIP(type\,I)}}(p) = -\frac{1}{4m}\epsilon^{\mu\rho\sigma\tau}\left\langle \frac{1}{p\cdot u}\hat{t}_{\rho}\xi_{\sigma\lambda}p^{\lambda}p_{\tau}\right\rangle, \qquad [1]$$

$$S^{\mu}_{\mathrm{SIP(type\,II)}}(p) = -\frac{1}{4m}\epsilon^{\mu\rho\sigma\tau}\left\langle \frac{1}{p\cdot u}u_{\rho}\xi_{\sigma\lambda}p^{\lambda}_{\perp}p_{\tau}\right\rangle, \qquad [2]$$

$$S^{\mu}_{\mu_B\mathrm{IP}}(p) = -\frac{1}{4m}\epsilon^{\mu\rho\sigma\tau}\left\langle \frac{T}{p\cdot u}u_{\rho}\partial_{\sigma}\left(\frac{\mu_B}{T}\right)p_{\tau}\right\rangle \qquad [3]$$

Thermal shear tensor $\xi^{\sigma\lambda} \equiv \frac{1}{2}[\partial^{\sigma}\left(\frac{u^{\lambda}}{T}\right) + \partial^{\lambda}\left(\frac{u^{\sigma}}{T}\right)]$

[1] Becattini, Buzzegoli, Palermo PLB 820, 136519 (2021); Buzzegoli PRC105, 044907 (2022)
[2] Liu, Yin PRD 104, 054043 (2021); JHEP 07, 188 (2021)
[3] Liu, Huang Sci. China Phys. Mech. Astron. 65, 272011 (2022),

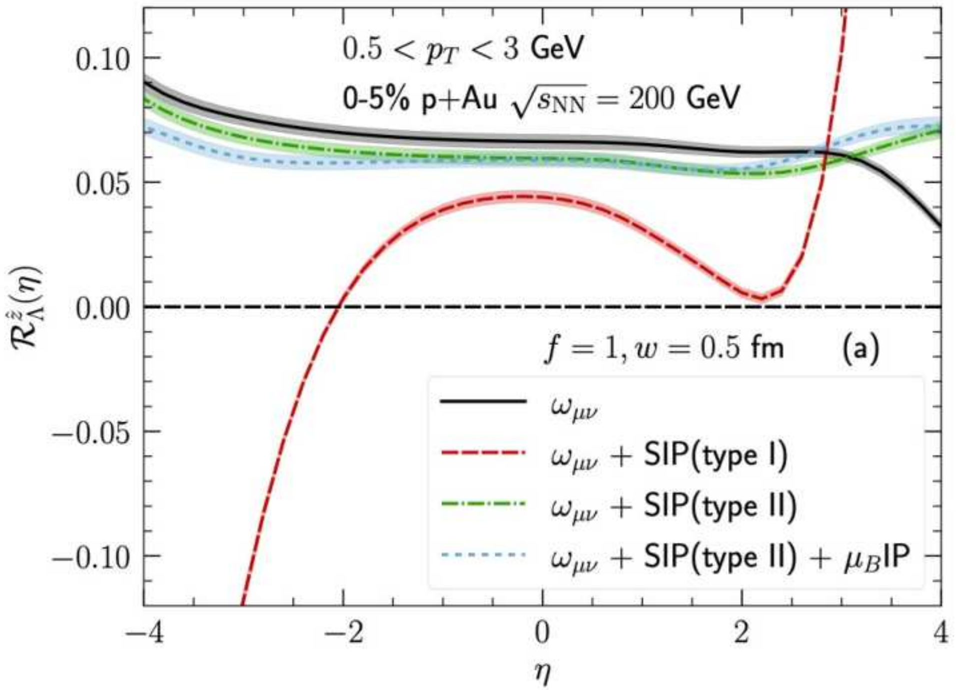

PR**C110** (2024) 054908

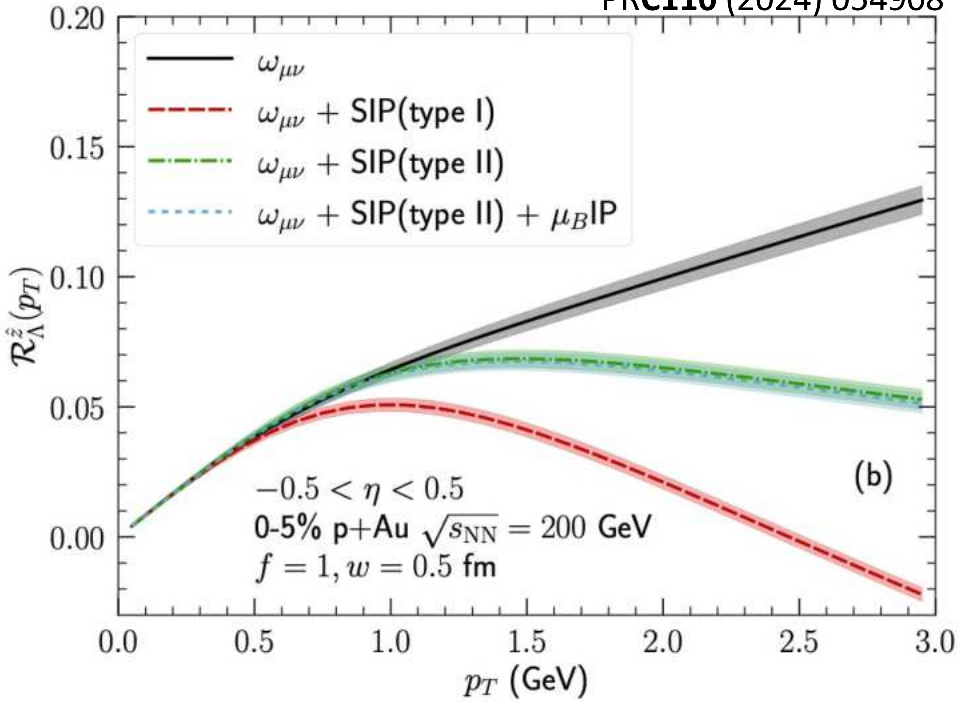

Hydrodynamics: simulation setup

The energy-momentum tensor is initialized as:

$$T^{\tau\tau} = e(\vec{x}_\perp, \eta_s)\cosh(f y_{\rm CM}(\vec{x}_\perp))$$
$$T^{\tau\eta} = \frac{1}{\tau_0} e(\vec{x}_\perp, \eta_s)\sinh(f y_{\rm CM}(\vec{x}_\perp))$$

with $y_{\rm CM}(\vec{x}_\perp)$ defined as:

$$y_{\rm CM}(\vec{x}_\perp) = {\rm arctanh}\left[\frac{T_A - T_B}{T_A + T_B}\tanh(y_{\rm beam})\right]$$

And f being a free parameter $\in$ [0, 1] such that:

$f = 0$: bjorken

$f = 1$:'matter

- **3D Initial conditions** with [1]
- Hydro: **MUSIC** [2] with **Lattice QCD EoS** [3]
- Particlization: **Cornelius** [4]
- **Parameters** most relevant to this study (varied later):
  - : nucleus size (default: 0.5 fm)
  - τ_0: hydrodynamization time (default: 1 fm/c)
  - η/s: shear viscosity (default: 0.08)
  - e_{sw}: freeze-out energy density (default: 0.5 GeV/fm³)
- **Freeze-out hypersurface spin polarization** via [5]:

$$S^{\mu}(p) \propto \epsilon^{\mu\rho\sigma\tau}\left(\partial_\sigma\left(\frac{u_\rho}{T}\right) - \partial_\rho\left(\frac{u_\sigma}{T}\right)\right)p_\tau$$

Thermal vorticity

- average: done over the freeze-out hypersurface

[1] Phys. Rev. C 102, 014909 (2020)
[2] Phys. Rev. C 82, 014903 (2010)
[3] Phys. Rev. C 100, 024907 (2019)

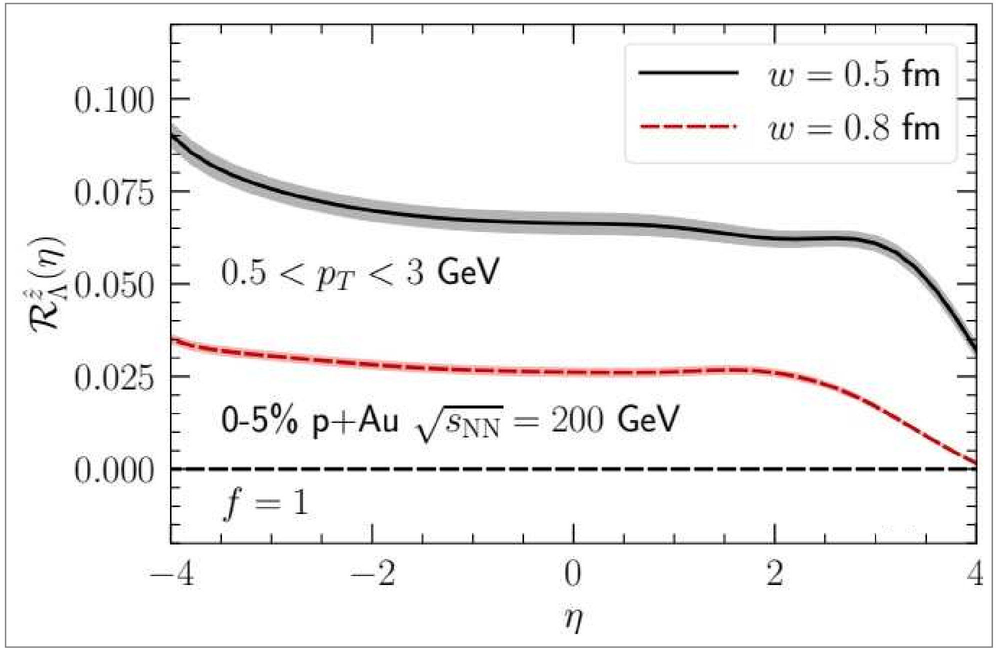

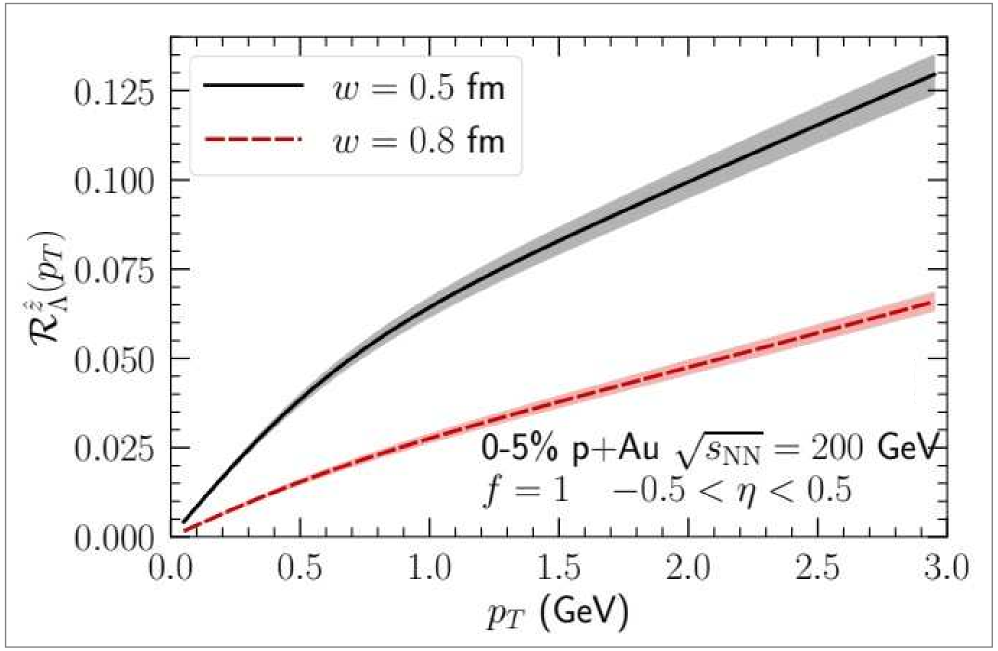

Figures from arXiv:2407.02212

Model dependence of the ring observable: hotspot size

- The **hotspot transverse size** w has a strong impact:
  - smaller hotspots → larger T gradients → larger thermal vorticity $\mathcal{R}^{\hat{z}}_{\Lambda}$
- Both a larger hotspot and a smaller f can reduce $\mathcal{R}^{\hat{z}}_{\Lambda}$ significantly
  - But: distinct p_T dependence of $f = 0$ or 1 breaks this degeneracy!
  - Negative derivative of $\mathcal{R}^{\hat{z}}_{\Lambda}$ with p_T only appears if $f = 0$

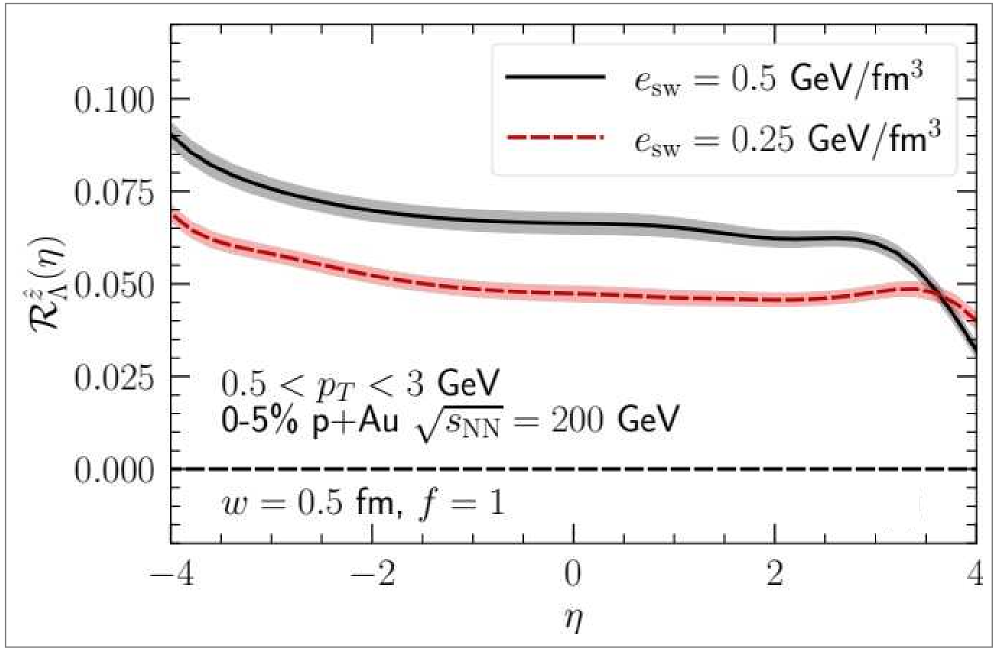

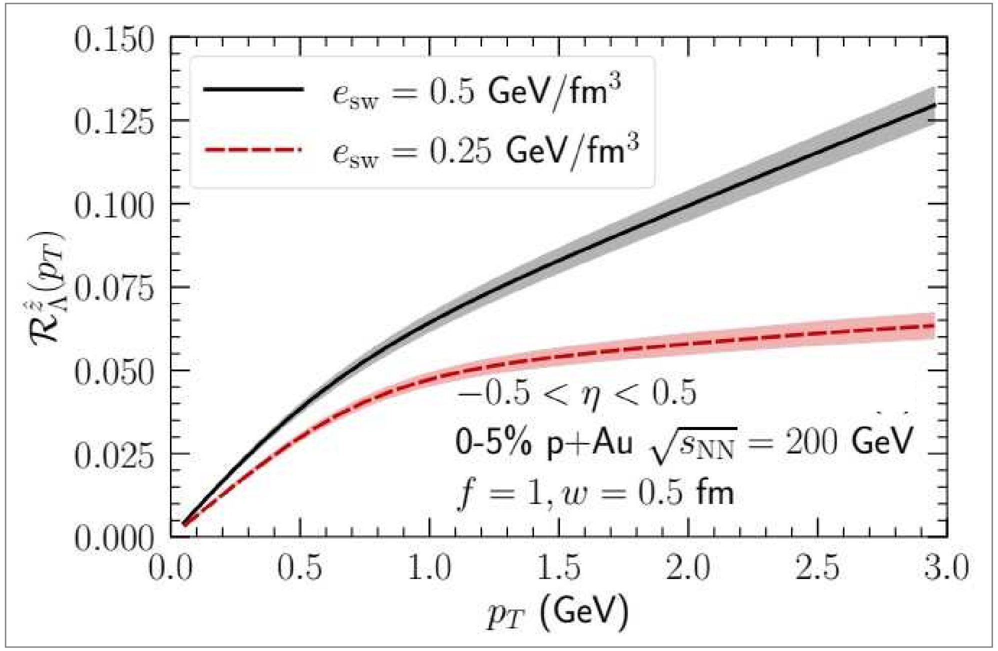

Figures from arXiv:2407.02212

Model dependence of the ring observable: freeze-out energy density

- The **freeze-out energy density** e_{sw} also impacts the outcome
  - Tested with 0.25 and 0.5 GeV / fm^3
  - Larger evolution time → vorticity relaxed to smaller values
  - Effect is most significant at larger momenta
- Other model variables were tested but have subdominant effects:
  - **Hydrodynamization time** τ_0
  - **Specific shear viscosity** η/s
- Even beyond: **coupling of hypersurface properties and spin** matters! $\mathcal{R}^{\hat{z}}_{\Lambda}$
  - Still significant theoretical uncertainty: see backup

From STAR BUR 2024-25 – statistical requirements

The statistical requirement to discover these toroidal vortex structures may be estimated by STAR's previous hyperon polarization measurements. The uncertainty on global polarization measurements $\delta\overline{P}_\Lambda \propto N_\Lambda^{-1/2} \cdot R_{\rm EP}^{-1}$, where N_Λ is the total number of hyperons in the analysis, and $R_{\rm EP}$ is the event plane resolution [7]. Because there is no event plane involved in the production plane polarization, on the other hand, the uncertainty on the ring observable goes as $\delta\overline{\mathcal{R}}_\Lambda^z \propto N_\Lambda^{-1/2}$. For the same-magnitude signal, then, $\overline{\mathcal{R}}_\Lambda^z$ enjoys an effective $R_{\rm EP}^{-2}$ "statistical advantage" over $\overline{P}_\Lambda$. Since STAR measured [104] $\overline{P}_\Lambda \approx 1\%$ at $\sqrt{s_{NN}} = 11$ GeV with 3.5σ significance, with the same number of hyperons in the analysis, we should be able to measure $\overline{\mathcal{R}}_\Lambda^z \sim 1\%$ with 7σ significance. The 11-GeV analysis involved 6M Λs, and we estimate 0.02 Λs per central $(0-10\%)$ p+Au collision at $\sqrt{s_{NN}} = 200$ GeV. Therefore, the 7σ measurement will require $6M/0.02 = 300M$ central p+Au collisions.

A 5-week run can discover/constrain

$$\underbrace{5\ \mathrm{w}}_{\text{run length}} \times 7\ \mathrm{d} \times 24\ \mathrm{h/d} \times 3600\ \mathrm{s/h} \times \underbrace{45\%}_{\text{RHIC/STAR efficiency}} = 1.4\ \mathrm{Ms\ data-taking}$$

$$1.4\ \mathrm{Ms} \times \underbrace{1000\ \mathrm{ev/s}}_{\text{event rate}} \times \underbrace{25\%}_{\text{trig, efficiency}} = 350\ \mathrm{Mevents}$$

STARNote **SN0819 : The STAR Beam Use Request for Run-24-25**
https://drupal.star.bnl.gov/STAR/starnotes/public/SN0819

c/o Joey Adams

Experimental issues

$$\overline{\mathcal{R}}_{\Lambda}^{\hat{z}} = 2\left\langle \frac{\vec{S}_{\Lambda}'\cdot(\hat{z}'\times\vec{p}_{\Lambda}')}{|\hat{z}'\times\vec{p}_{\Lambda}'|} \right\rangle_{\phi} = \frac{8}{\pi\alpha}\left\langle \sin\left(\phi_p - \phi_\Lambda\right)\right\rangle$$

Challenge: large topological dependence of efficiency

- artifacts *complicated* and ~10% (or more)
- will affect *any* tracking detector
- ***must** flip B-field* to cancel artifact

STAR PRC104 (2021) L061901

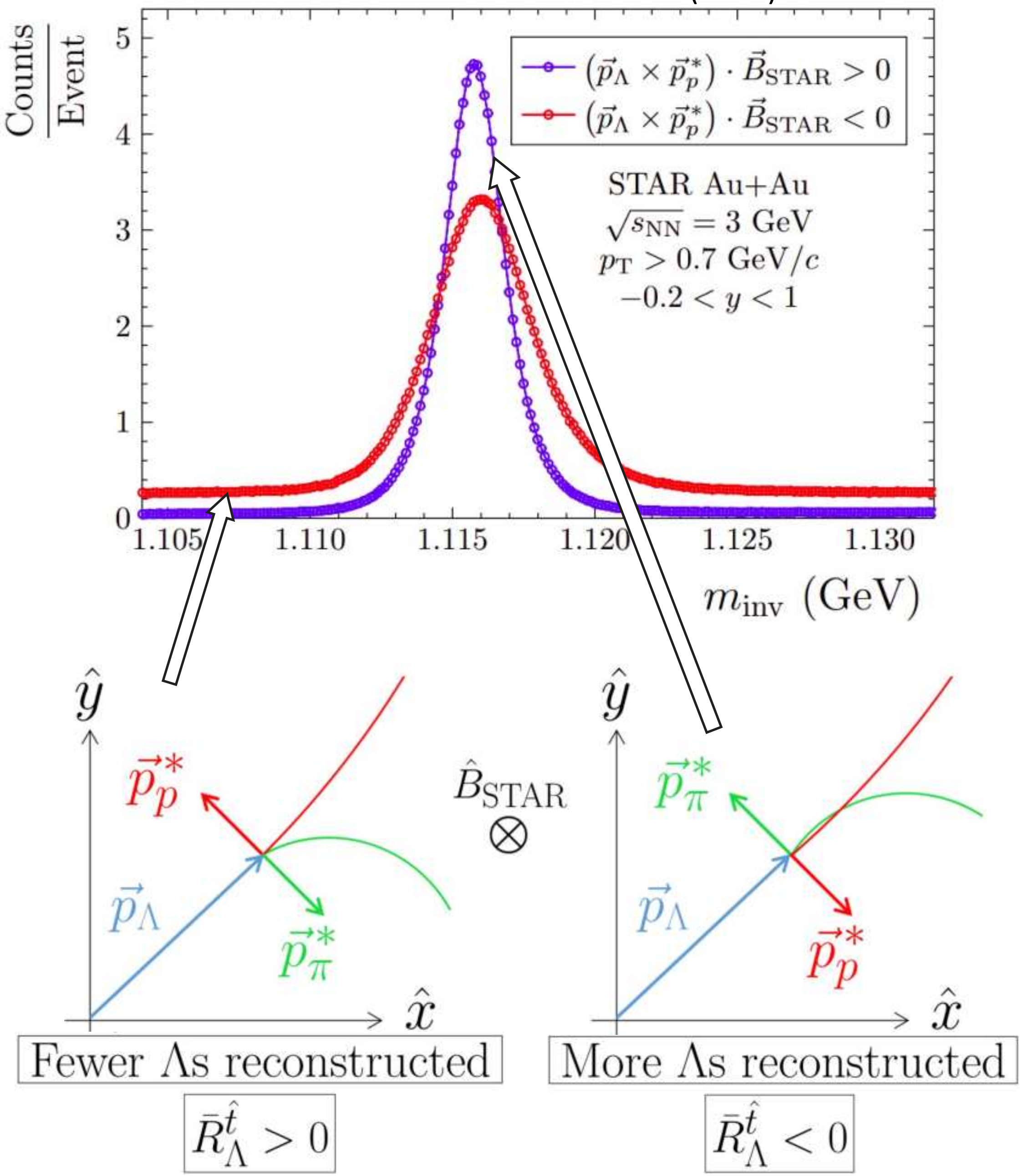

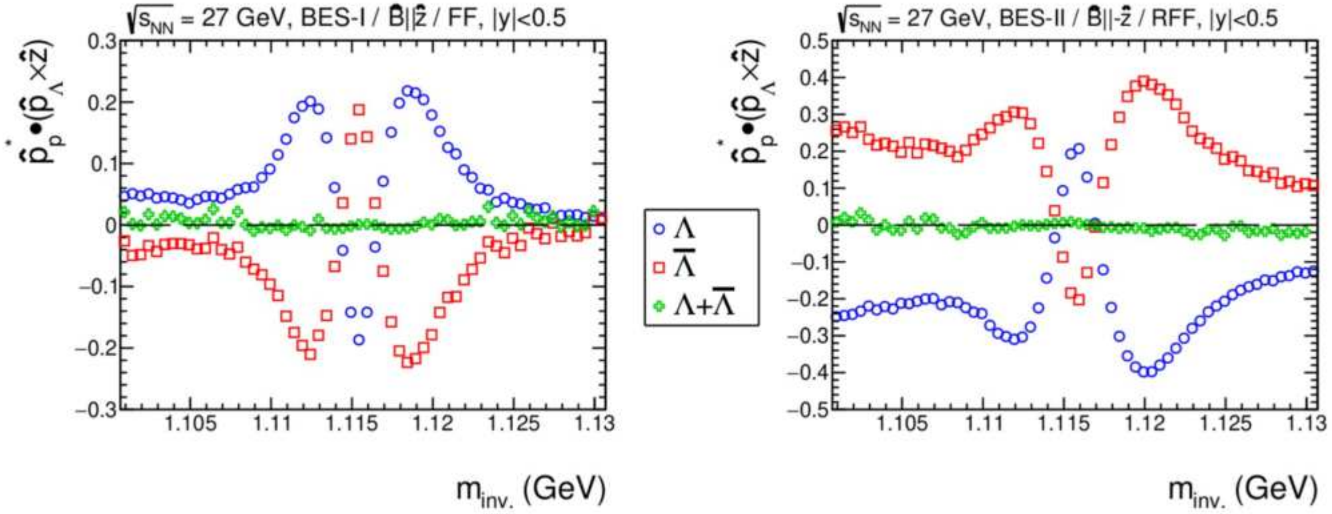

STARNote **SN0819 : The STAR Beam Use Request for Run-24-25**
https://drupal.star.bnl.gov/STAR/starnotes/public/SN0819

Experimental issues

STAR PRC104 (2021) L061901

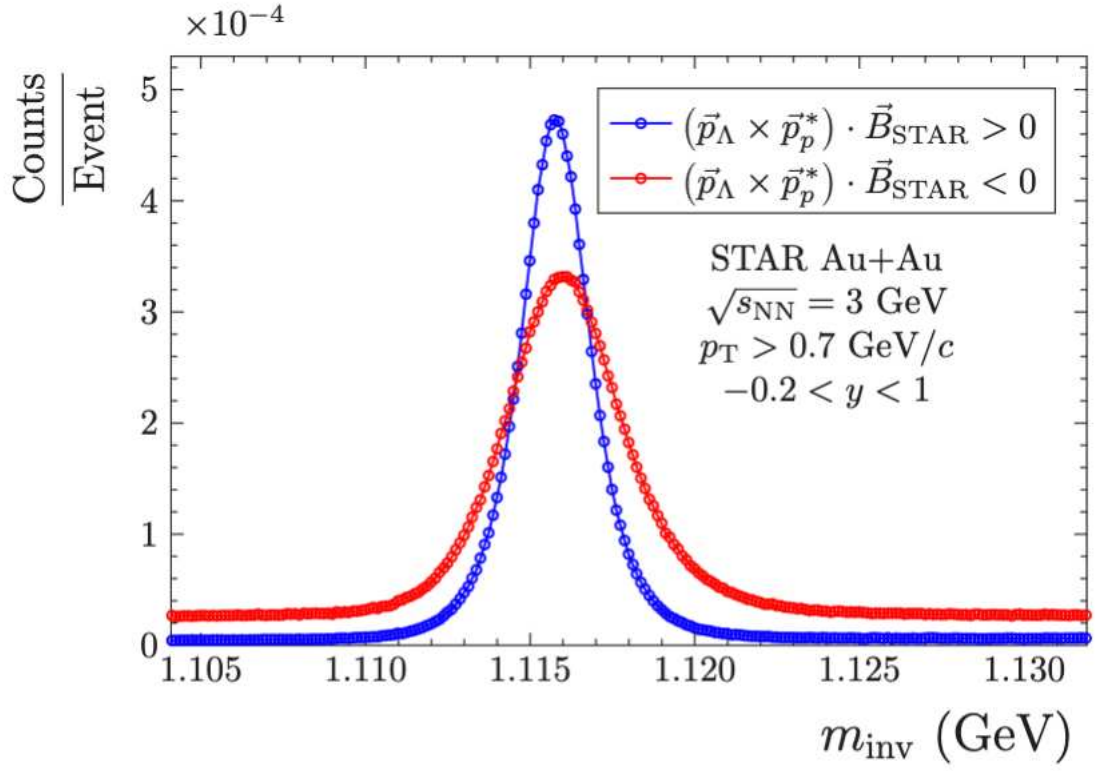

FIG. 1. The measured m_{inv} distributions of two classes of Λ-hyperon decays: "right" decays in blue, with $(\vec{p}_\Lambda \times \vec{p}_p^*) \cdot \vec{B}_{\text{STAR}} > 0$, and "left" decays in red, with $(\vec{p}_\Lambda \times \vec{p}_p^*) \cdot \vec{B}_{\text{STAR}} < 0$. The "right" decay class has a notably sharper m_{inv} distribution than the "left" decay class, and this is due to the effects of daughter tracks crossing in the STAR TPC with $\vec{B}_{\text{STAR}} || -\hat{z}$. The opposite pattern is obtained by flipping the sign of $\vec{B}_{\text{STAR}}$ or by reconstructing $\bar{\Lambda}$ hyperons.

Experimental issue – requirement to flip field

STARNote **SN0819 : The STAR Beam Use Request for Run-24-25**
https://drupal.star.bnl.gov/STAR/starnotes/public/SN0819

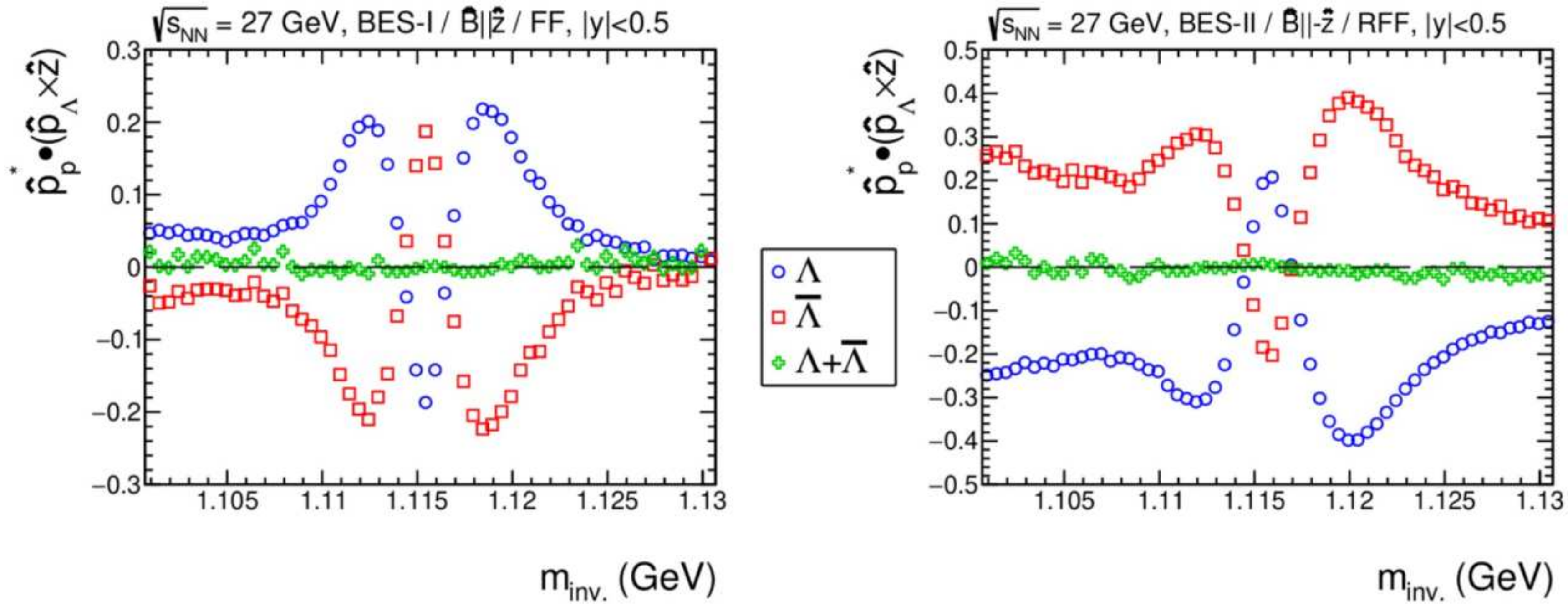

Figure 104: Production-plane polarization (modulo an overall scaling by $\frac{8\pi}{\alpha_\Lambda}$) for Λ (blue) and $\overline{\Lambda}$ (red) candidates, as a function of invariant mass. The data comes from STAR measurements of Au+Au collisions at $\sqrt{s_{NN}}$ in the BES-I (left) and BES-II (right) campaigns. STAR's solenoidal magnetic field was directed to the West and East, respectively, for these two datasets. For the BES-I data, hyperon candidates were identified with "standard" topological cuts, whereas the candidates shown in BES-II were identified using the new KFParticle package.

f parameter and *global* polarization

Ryu, Jupic, Shen: 2106.08125

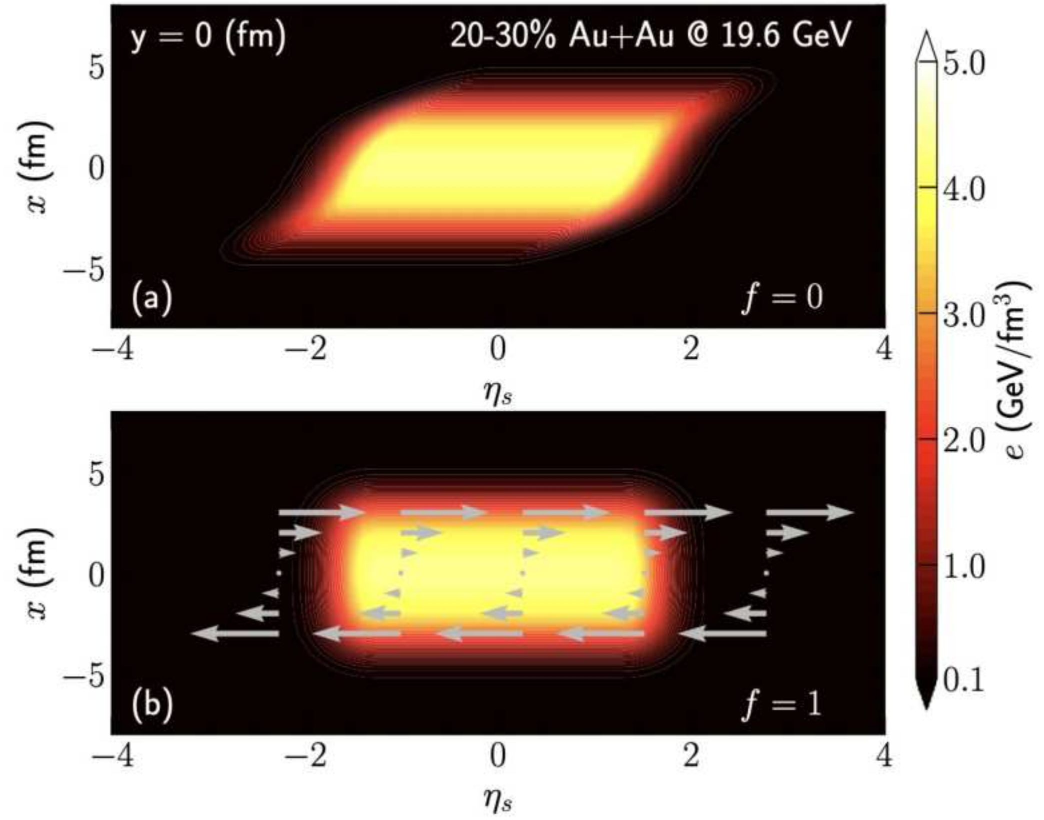

FIG. 1. Color contours show the initial energy density distributions in the $x - \eta_s$ plane for 20-30% Au+Au collisions at 19.6 GeV with the longitudinal rapidity fraction $f = 0$ (a) and $f = 1$ (b). The grey arrows in panel (b) indicate the non-zero initial longitudinal flow u^η with $y_L = y_{CM}$ in Eqs. (13) and (14). $u^\eta = 0$ in panel (a).

Chun Shen

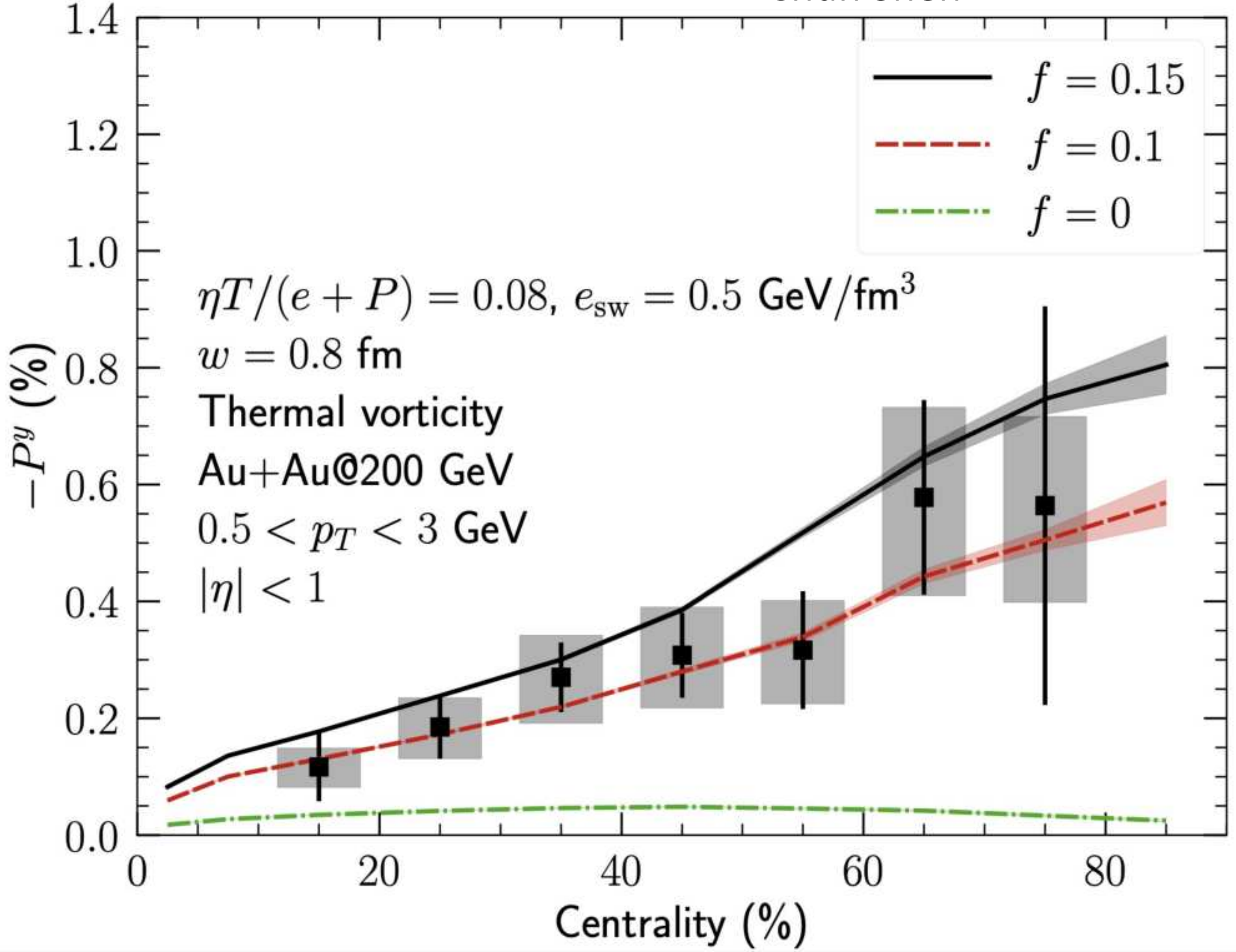

It is unclear to me that f will be the same in p+A

Reminder from 1970's (through 2010's)

production-plane polarization in p+A collisions.

- Same observable as ours!
- high-x signal
- ~independent of target (p, Be, C, Cu, W)
- ~independent of energy (only measured to ~40 GeV)
- odd in rapidity for p+p, but also p+A
- no signal for anti-Lambdas

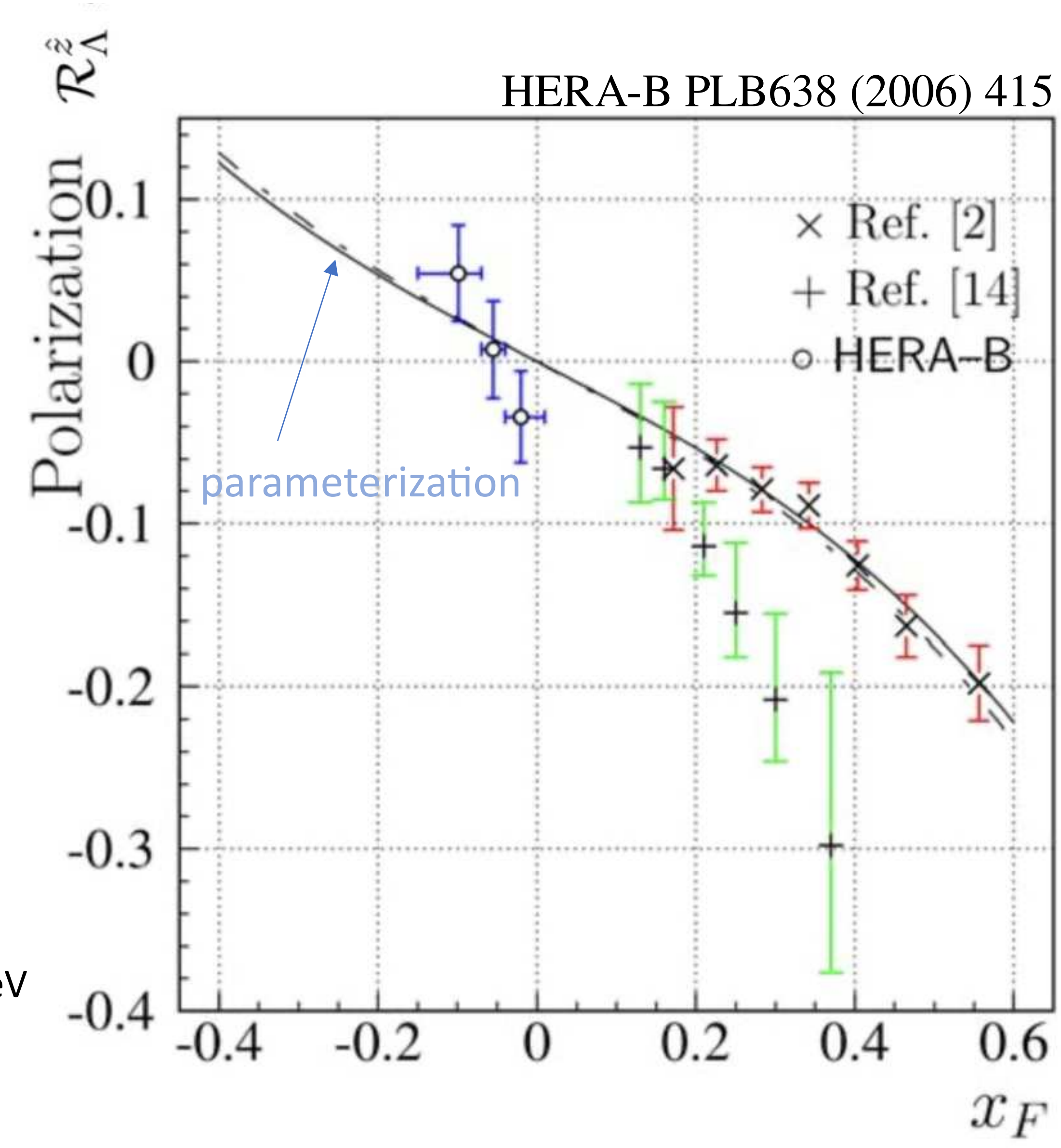

+	NA48 p+N(?)	sqrt(sNN) = 29 GeV
x	E799 p+Be	sqrt(sNN) = 39 GeV
○	HERA-B p+W,C	sqrt(sNN) = 41.6 GeV